2.4. Cell culture and transfection procedure

B16BL6, a murine melanoma cell line, was maintained in Dulbecco's modified Eagle's medium (DMEM) (Nissui Pharmaceutical Co. Ltd, Tokyo, Japan) containing 10 mM glutamine, 100 units/ml penicillin and 100 μg/ml streptomycin supplemented with 10% heat-inactivated fetal bovine serum (FBS) in a 5% CO_2 air incubator at 37 °C. The cells were maintained in exponential growth. Two luciferase plasmids (*Photinus* (firefly) luciferase, pGL-3 and *Renilla* (sea pansy) luciferase, pRL-TK) were used as reporter and control genes, respectively, by a reported transfection protocol with modifications (Elbashir et al., 2001). The cells were seeded in 24-well plates at a density of 5.0×10^4 cells/well 24 h before the transfection was carried out. Prior to transfection, the medium was removed. The cells were co-transfected with pDNA/siRNA/TFL-3 lipoplex or with the mixture of pDNA/TFL-3 lipoplex and siRNA/TFL-3 lipoplex in OPTIMEM I (500 μl/well). The siRNA concentrations for transfection were 1.5625, 3.125, 6.25, 12.5, 25, 50 and 100 nM. The transfection medium was exchanged for culture medium (500 μl) after 4 h. All experiments were performed in triplicate and repeated at last twice.

2.5. Dual-luciferase reporter assay

Cells were harvested 20 h after transfection and lysed by passive lysis buffer (100 μl/well), according to the instruction of the Dual-Luciferase Reporter Assay System (Promega) with modifications. The luciferase activities of the samples were measured using a luminometer (BLR-301, Aloka, Tokyo, Japan), with a delay time of 2 s and an integrate time of 10 s. The volumes of sample (20 μl), luciferase assay reagent II (100 μl), and Stop & Glo Reagent (100 μl) were reduced to half the amount when the activity of the reporter or control gene saturated the luminometer. The inhibitory effects generated by siRNA were expressed as normalized ratios between the activities of reporter (firefly) luciferase gene and control (sea pansy) luciferase gene (Elbashir et al., 2001; Xu et al., 2003).

2.6. Effect of non-transcriptional pDNA on the gene-silencing effect of siRNA

Non-transcriptional pDNA, pGEM-luc, was purchased from Promega (WI, USA). pDNA (pGL-3 and pRL-TK, 0.5 μg)/TFL-3 lipoplex (2.5 nmol) was prepared in OPTIMEM I as described above. siRNA/pDNA (pGEM-luc)/TFL-3 lipoplex was also prepared in OPTIMEM I as described above. For preparation of the siRNA/pDNA/TFL-3 lipoplex, siRNA was kept at 25 nM and pDNA (pGEM-luc) was varied from 0.0625 to 0.5 μg. The cells were co-transfected as described above and the dual-luciferase assay was performed.

2.7. Amount of siRNA transferred into the cells by transfection

Lipoplexes containing fluorescence (FAM)-labeled siRNA, custom synthesized by Hokkaido System Science, were transfected as described above. At 4 h after transfection, the cells were washed twice with ice-cold PBS and treated with 100 μl/well of a lysis buffer (ice-cold PBS containing 2% (w/v) Triton-X 100, 1 μl of protease inhibitor (×100 protease inhibitor cocktail (50 mM 4-(2-aminoethyl)benzenesulfonyl fluoride (AEBSF), 15 μM aprotinin (from bovine lung), 100 μM E-64, 100 μM leupeptin hemisulfate salt, 50 μM EDTA, Nacalai Tesque, Kyoto, Japan))) on ice for 1 h. The cell lysate was collected and centrifuged (20,000 × *g*, 5 min, 4 °C) to give a clear supernatant. The fluorescence of samples was determined using a fluorometer (F-4500, Hitachi, Tokyo, Japan). The protein content in the samples was determined with the DC protein assay kit (Bio-Rad Laboratories, CA, USA). The data are expressed as the fluorescence/mg of protein.

2.8. Confocal microscopy

The cells were transfected with lipoplexes containing FAM-labeled siRNA and rhodamine-labeled TFL-3 (supplied by Daiichi Pharmaceutical). For preparation of the siRNA/pDNA/TFL-3 lipoplex, FAM-labeled siRNA (25 pmol), pDNA (2 μg) and rhodamine-labeled TFL-3 (5 nmol) were mixed, and the total volume was adjusted to 250 μl with OPTIMEM I. For preparation of the siRNA/TFL-3 lipoplex, FAM-labeled siRNA (25 pmol) and rhodamine-labeled TFL-3 (2.5 nmol) were mixed, and the total volume was adjusted to 250 μl with OPTIMEM I. For preparation of the pDNA/TFL-3 lipoplex, pDNA (2 μg) and rhodamine-labeled TFL-3 (2.5 nmol) were mixed, and the total volume was adjusted to 250 μl with OPTIMEM I. At 4 h after transfection, the cells were washed twice with ice-cold PBS. Then the cells were immediately examined using a Zeiss LSM5 inverted confocal laser scanning microscope (Carl Zeiss, Oberkochen, Germany) without fixation. FAM-siRNA was imaged using a 488 nm filter for excitation and a 510–530 nm filter for emission, respectively. Rhodamine-labeled TFL-3 was imaged using a 540 nm filter for excitation and a 650 nm filter for emission, respectively.

2.9. Statistics

All values are expressed as the mean ± S.D. Statistical analysis was performed with a two-tailed unpaired *t*-test using GraphPad InStat software (GraphPad Software, CA, USA). The level of significance was set at $p < 0.05$.

3. Results

3.1. Characterization of lipoplexes

After preparation, all lipoplexes (siRNA/pDNA/TFL-3, siRNA/TFL-3 and pDNA/TFL-3) were checked for free nucleic acids by an agarose electrophoresis. No free siRNA and/or pDNA were detected (not shown). The mean diameters and zeta potentials of all lipoplexes were analyzed (Table 1). The mean particle sizes of siRNA/pDNA/TFL-3 lipoplexes produced by the co-preparation method (Method I) increased with

Table 1
Characterization of the lipoplexes

siRNA/pDNA/TFL-3			Diameter (nm)	Zeta potential (mV)
siRNA (μM)	pDNA (μg/ml)	TFL-3 (μM)		
Co-preparation (Method I)				
12.5	2	20	305.3	+29.26
25	2	20	374.2	+29.07
50	2	20	392.4	+29.44

siRNA/TFL-3		Diameter (nm)	Zeta potential (mV)
siRNA (μM)	TFL-3 (μM)		
Separate preparation (Method II)			
12.5	10	301.9	+36.59
25	10	279.9	+37.13
50	10	307.7	+30.35

pDNA/TFL-3		Diameter (nm)	Zeta potential (mV)
pDNA (μg/ml)	TFL-3 (μM)		
Separate preparation (Method II)			
20	10	317.5	+27.54

TFL-3 (μM)	Diameter (nm)	Zeta potential (mV)
Control		
10	266.5	+37.49

Mixture of pGL-3 and pRL-TK (9:1, w/w) was used as pDNA. siRNA for *Renilla* (firefly) luciferase was used.

increasing amount of siRNA, while zeta potential values did not change. The mean particle size of the siRNA/TFL-3 complexes produced by separate preparation (Method II) did not change regardless of the amount of siRNA, while the zeta potential values of these lipoplexes decreased with increasing amounts of siRNA. The mean diameter of TFL-3 liposomes increased by complexing with pDNA (separate preparation according to Method II), while the zeta potential value decreased.

3.1.1. Suppression of Renilla (firefly) luciferase expression in B16BL6 cells

The ratio of firefly and sea pansy luciferase activities was determined after co-transfection (Fig. 1). The siRNA in the lipoplexes produced by co-preparation (Method I) was far more effective than the siRNA in the separately prepared lipoplexes (Method II). Even at a concentration as low as 1.5625 nM, the siRNA in the co-prepared lipoplexes induced more than 80% inhibition. To obtain a similar inhibition with the separately prepared lipoplexes, more than 100 nM of siRNA was required. The gene-silencing effect of siRNA in the lipoplexes produced by co-preparation was 60-fold higher than that in the lipoplexes produced by separate preparation. It is to be noted that the activities of sea pansy luciferase (control) were similar throughout the experiments (Table 2). Furthermore, unrelated siRNA did not show any significant gene-silencing effect at any of the applied concentrations regardless of the preparation method (data not shown).

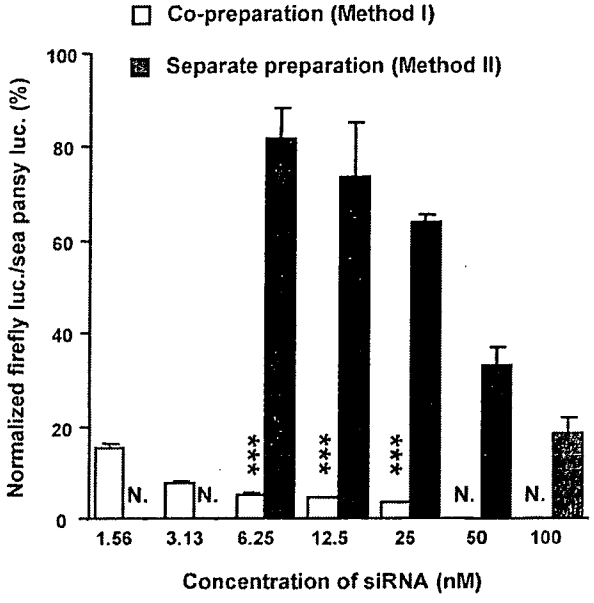

Fig. 1. Effect of the lipoplex preparation method (Method I or Method II) on the gene-silencing potential of transfected siRNA. Results presented are from three independent experiments. $^{***}p < 0.005$; N., not determined.

3.2. Amount of siRNA associated with the cells

To evaluate whether intracellular uptake of siRNA was related to the induced gene-silencing effect, the amount of siRNA transferred into the cells was determined by using FAM-labeled siRNA. The amount of siRNA associated with the cells increased with increasing the siRNA concentration (Fig. 2). Although the amount of siRNA transferred by lipoplexes produced by co-preparation was larger than that transferred by separately prepared lipoplexes, there was no significant difference in the amount of transferred siRNA.

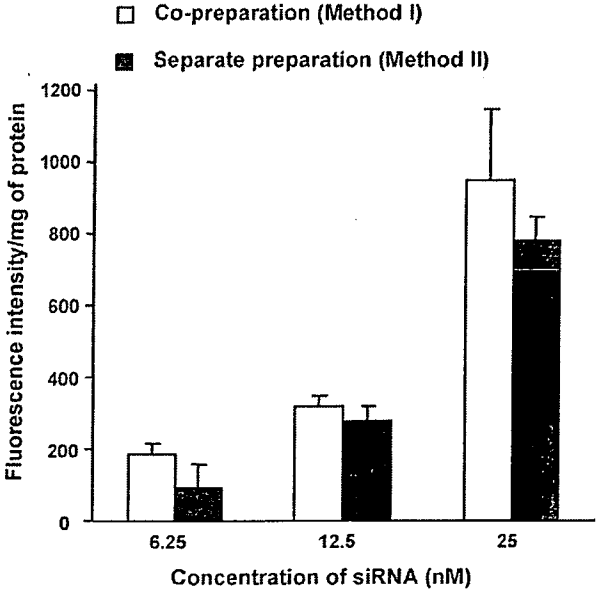

Fig. 2. Amount of siRNA associated with the cells following transfection. Cells were incubated with lipoplexes containing a fluorescently labeled siRNA. After 4 h the cells were lysed and fluorescence in the lysates was quantified. For details see Section 2. Results presented are from three independent experiments.

Table 2
Firefly and sea pansy luciferase activities in B16BL6 cells

	siRNA concentration							
	0 nM (Control)	1.56 nM	3.13 nM	6.25 nM	12.5 nM	25 nM	50 nM	100 nM
Co-preparation (Method I)								
Firefly luciferase activity (cpm)	266137.3 ± 41567.5	37204.3 ± 1214.6	19677.5 ± 1974.9	15127.3 ± 1869.0	12394.3 ± 1175.7	9367.7 ± 2710.1	N.	N.
Sea pansy luciferase activity (cpm)	4187.8 ± 491.4	4256.3 ± 198.1	4583.3 ± 321.9	5270.0 ± 349.8	4562.7 ± 299.2	3823.0 ± 1039.9	N.	N.
Separate preparation (Method II)								
Firefly luciferase activity (cpm)	256359.2 ± 29810.1	N.	N.	180235.5 ± 13314.2	155066.8 ± 16901.1	144200.5 ± 19648.0	44268.8 ± 4925.7	25888.0 ± 2866.2
Sea pansy luciferase activity (cpm)	5141.4 ± 728.5	N.	N.	5621.8 ± 518.5	5867.0 ± 772.4	5893.3 ± 215.9	4216.5 ± 380.9	3919.8 ± 343.6

The luciferase activities were determined according to the method described in Section 2. Results presented are from three independent experiments. N., not determined.

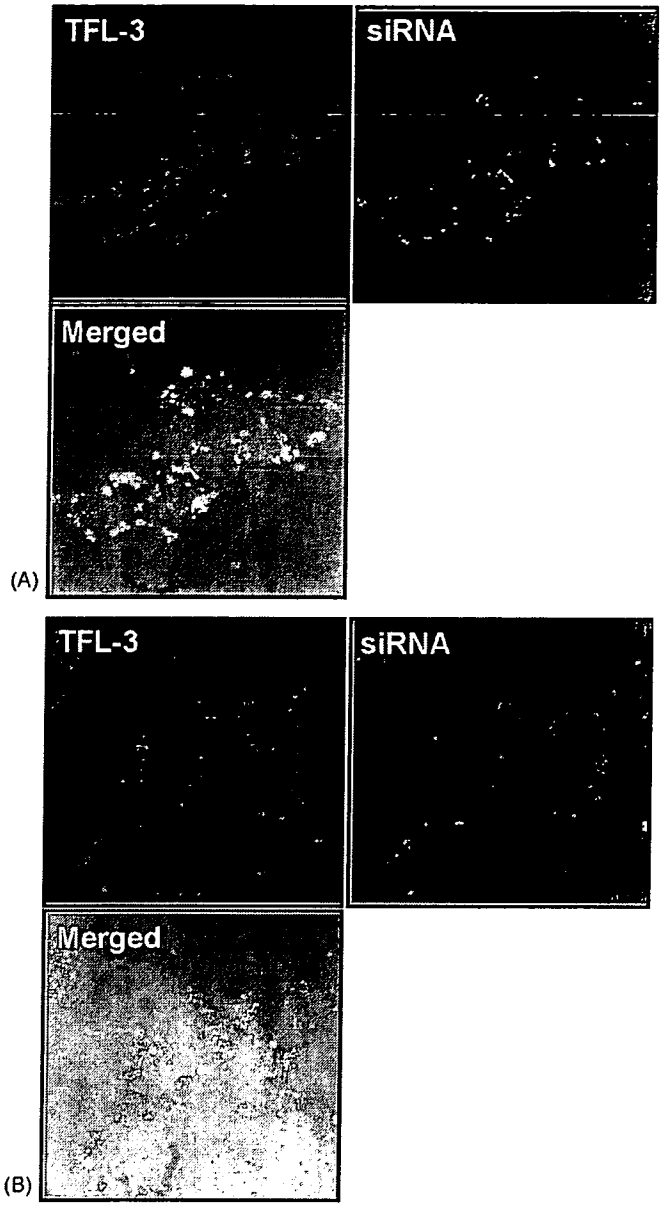

Fig. 3. Intracellular distribution of the lipoplexes produced by the (A) co-preparation method and (B) separate preparation method. Cells were incubated for 4 h with lipoplexes containing rhodamine-labeled TFL and FAM-labeled siRNA and immediately thereafter observed by confocal microscopy. Rhodamine, red; FAM, green.

3.3. Intracellular distribution of lipoplexes

The intracellular trafficking of the lipoplexes containing FAM-labeled siRNA, pDNAs and rhodamine-labeled TFL-3 was examined by means of confocal microscopy. Pictures were taken immediately after the transfection was terminated. Fig. 3A shows the intracellular distribution of lipoplexes (FAM-siRNA/pDNA/rhodamine-TFL-3) produced by co-preparation (Method I). Co-localization of siRNA and TFL-3 (merging green and red producing yellow) was observed. Fig. 3B shows the intracellular distribution of lipoplexes (FAM-siRNA/TFL-3 and pDNA/rhodamine-TFL-3) produced by separate preparation (Method II). siRNA (green) and TFL-3 (red) can be distin-

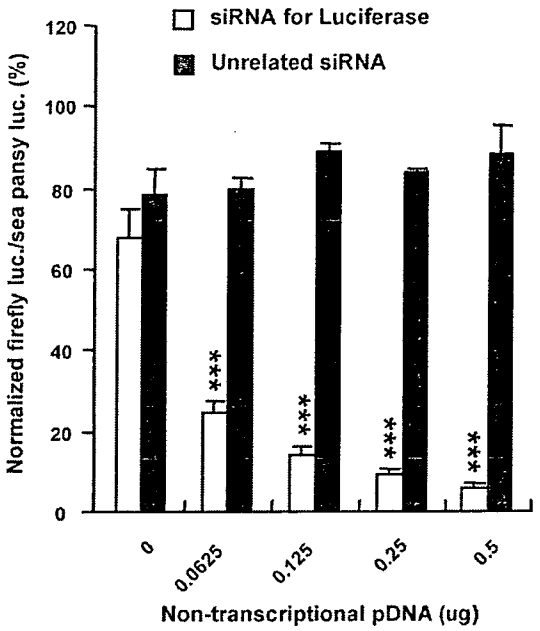

Fig. 4. Effect of the presence of non-transcriptional pDNA in the lipoplex on the gene-silencing potential of siRNA. See Section 2 for details. Results presented are from three independent experiments. $^{***}p < 0.005$.

guished as individual spots in the cells. It should be noted that the amount of rhodamine-labeled TFL-3 for the preparation of lipoplexes with siRNA and pDNA was twice as large as that for the preparation of lipoplexes with pDNA. The fluorescence intensity of siRNA/pDNA/rhodamine-labeled TFL-3 lipoplexes will therefore be higher than that of pDNA/rhodamine-labeled TFL-3.

3.4. Induction of the gene-silencing effect of siRNA by a non-transcriptional pDNA

From the results of the confocal microscopy, we assumed that pDNA in the lipoplexes produced by co-preparation (Method I) has somehow the ability to bring the siRNA to an optimal position in the cytoplasm allowing it to induce a higher gene-silencing effect. To test this, we prepared lipoplexes containing a non-transcriptional pDNA and siRNA for *Renilla* (firefly) luciferase and incubated them with cells after transfection with pDNAs/TFL-3 lipoplexes. Inhibition of gene expression increased with the amount of non-transcriptional pDNA (Fig. 4). It is noteworthy that the sea pansy luciferase activities (control) were similar throughout the experiments (data not shown).

4. Discussion

Gene silencing by siRNA can be assayed by studying its inhibitory effect on the expression of an exogenous gene co-transfected into the cell simultaneously with the siRNA. In this study, we compared two principally different approaches for this co-transfection, either by accommodating the pDNA in the same complex together with the siRNA (Method I), or by incorporating the pDNA and the siRNA in two separate complexes (Method II).

The siRNA lipoplexes produced by Method I showed a much stronger reporter-gene silencing effect than those produced by Method II (Fig. 1). This observation clearly calls for caution when drawing conclusions concerning the activity of synthesized siRNAs and/or the effectiveness of the delivery system used. It may be necessary to first establish a reliable evaluation method. Aiming at an endogenous gene or a stably expressed exogenous gene rather than at a transiently expressed gene would probably provide more reliable results.

During transfection with lipoplexes produced by Method II, one lipoplex might competitively inhibit the cellular uptake of the other. The consequently lower amount of transferred siRNA might be insufficient to silence the larger exogenous gene expression. In addition, lower target gene-expression due to lower cellular uptake of pDNA might lead to an over-estimation of the gene-silencing effect by transferred siRNA. We observed, however, that the expression of the control gene (*Renilla* (sea pansy) luciferase) as well as the amount of siRNA associated with the cells were nearly constant, irrespective of the preparation method (Fig. 2). This strongly suggests that the lower gene-silencing effect of lipoplexes prepared by Method II cannot be attributed to mutually competitive inhibition of the cellular uptake of pDNA or siRNA.

Although pDNA and siRNA both have anionic phosphodiester backbones with identical negative charge/nucleotide ratios and should therefore readily interact electrostatically with cationic liposomes to form lipoplexes, they are very different from each other in terms of molecular weight and molecular topography. This may bring along potentially important consequences. The resulting lipoplexes, i.e. complexes with only siRNA or only pDNA or complexes with both siRNA and pDNA, are each likely to display unique physicochemical properties and, consequently, to lead to different types of interaction with the cells. In fact, in the case of pDNA, it has been reported that larger lipoplexes tend to give better transfection results than smaller lipoplexes (Kreiss et al., 1999; Ross and Hui, 1999; Simberg et al., 2001; Almofti et al., 2003). In contrast to the pDNA delivery, no difference in gene-silencing potential was observed between smaller lipoplexes (50–100 nm) and larger lipoplexes (200–600 nm) (Spagnou et al., 2004). In our experiments we observed no significant differences between complexes prepared by the two different methods in terms of particle diameter and zeta potential (Table 1), presumably due to the small amounts of siRNA and pDNA that were used to form the lipoplexes. We therefore believe that it is also not a difference in physicochemical properties of the lipoplexes that is the major cause of the different gene-silencing effects of siRNA observed in our study. This view is supported by the constant values of the control exogenous gene expression levels we observed and by the similar amounts of siRNA associated with the cells, irrespective of the preparation method.

It is generally assumed that the cellular entry and intracellular trafficking of siRNA are the key processes in determining the efficiency of gene-silencing effects with exogenous siRNA following transfection (Hammond et al., 2000; Martinez et al.,

2002; Schwarz et al., 2002). Our confocal microscopy study demonstrated that the siRNA delivered by siRNA/pDNA/TFL-3 lipoplexes co-localized in the cell with TFL-3 (Fig. 3A), implying that siRNA also co-localized with pDNA. By contrast, the observation that the siRNA delivered by siRNA/TFL-3 lipoplexes did not co-localize with pDNA/rhodamine-labeled TFL-3 lipoplexes (Fig. 3B) indicated that siRNA and pDNA localize separately after entry in the cells. These observations may indicate that the cellular entry and the intracellular trafficking of the siRNA/pDNA/TFL-3 lipoplexes differ from that of other lipoplexes (siRNA/TFL-3 and pDNA/TFL-3). We recently reported that the cellular entry of pDNA/TFL-3 lipoplex occurs via the endocytosis pathway (Almofti et al., 2003). The mechanisms of siRNA entry into the cells and their intracellular trafficking mediated by the TFL-3 have not yet been established, however. Miller and co-workers (Keller et al., 2003; Spagnou et al., 2004) demonstrated that intracellular uptake and localization of siRNA and pDNA complexed in their carrier system (CDAN (N^1-cholesteryloxycarbonyl-3,7-diazanonane-1,9-diamine)/DOPE (dioleoylphosphatidylethanolamine) liposomes) differ substantially between siRNA lipoplexes and pDNA lipoplexes. Uptake and intracellular trafficking of siRNA/pDNA/TFL-3 lipoplex likewise may differ from those of siRNA/TFL-3 and pDNA/TFL-3 lipoplexes.

Although we do not yet understand the underlying mechanism, we clearly demonstrated that pDNAs, also if non-transcriptional, can increase the gene-silencing effect of the associated siRNA provided that it is present with the siRNA in the same lipoplex (Figs. 1 and 4). Recently, Schiffelers et al. (2004) reported similar findings in *in vivo* experiments. They compared co-injection (pDNA and siRNA injected simultaneously) with sequential injections (siRNA injected 2 h after pDNA) with respect to exogenous-gene-silencing potential siRNA-RGD-PEI-PEG-nanocomplex, targeted to tumor neovasculature expressing integrins; *in vivo*. siRNA was efficiently delivered by the nanocomplex using either injection protocol, but the induced gene-silencing effect was lower with the sequential injection protocol than with the co-injection protocol. The pDNA in the same lipoplex with siRNA may guide the siRNA to the correct position to function in the cells. This may open up new perspectives for gene therapy by means of pDNA and siRNA. The silencing of (aberrant) genes linked to human disorders and at the same time expressing genes producing a therapeutic protein with specific functions in the same cells may synergistically increase the efficacy of the gene therapy, when lipoplexes containing both a pDNA encoding functional gene and a gene-specific siRNA are injected. To achieve this ambitious goal suitably targeted carrier systems will have to be developed which are capable of delivering their nucleic acid cargos to target tissues or cells.

Acknowledgements

We thank Dr. G.L. Scherphof for his help in writing the manuscript. This study was supported in part by Health and Labour Sciences Research Grants on Advanced Medical Technology from the Ministry of Health, Labour and Welfare.

References

Almofti, M.R., Harashima, H., Shinohara, Y., Almofti, A., Li, W., Kiwada, H., 2003. Lipoplex size determines lipofection efficiency with or without serum. Mol. Membr. Biol. 20, 35–43.

Bitko, V., Musiyenko, A., Shulyayeva, O., Barik, S., 2005. Inhibition of respiratory viruses by nasally administered siRNA. Nat. Med. 11, 50–55.

Elbashir, S.M., Harborth, J., Lendeckel, W., Yalcin, A., Weber, K., Tuschl, T., 2001. Duplexes of 21-nucleotide RNAs mediate RNA interference in cultured mammalian cells. Nature 411, 494–498.

Hammond, S.M., Bernstein, E., Beach, D., Hannon, G.J., 2000. An RNA-directed nuclease mediates post-transcriptional gene silencing in *Drosophila* cells. Nature 404, 293–296.

Keller, M., Harbottle, R.P., Perouzel, E., Colin, M., Shah, I., Rahim, A., Vaysse, L., Bergau, A., Moritz, S., Brahimi-Horn, C., Coutelle, C., Miller, A.D., 2003. Nuclear localization sequence templated non-viral gene delivery vectors: investigation of intracellular trafficking events of LMD and LD vector systems. Chembiochem 4, 286–298.

Khoury, M., Louis-Plence, P., Escriou, V., Noel, D., Largeau, C., Cantos, C., Scherman, D., Jorgensen, C., Apparailly, F., 2006. Efficient new cationic liposome formulation for systemic delivery of small interfering RNA silencing tumor necrosis factor alpha in experimental arthritis. Arthritis Rheum. 54, 1867–1877.

Kikuchi, A., Aoki, Y., Sugaya, S., Serikawa, T., Takakuwa, K., Tanaka, K., Suzuki, N., Kikuchi, H., 1999. Development of novel cationic liposomes for efficient gene transfer into peritoneal disseminated tumor. Hum. Gene Ther. 10, 947–955.

Kreiss, P., Cameron, B., Rangara, R., Mailhe, P., Aguerre-Charriol, O., Airiau, M., Scherman, D., Crouzet, J., Pitard, B., 1999. Plasmid DNA size does not affect the physicochemical properties of lipoplexes but modulates gene transfer efficiency. Nucleic Acids Res. 27, 3792–3798.

Landen Jr., C.N., Chavez-Reyes, A., Bucana, C., Schmandt, R., Deavers, M.T., Lopez-Berestein, G., Sood, A.K., 2005. Therapeutic EphA2 gene targeting in vivo using neutral liposomal small interfering RNA delivery. Cancer Res. 65, 6910–6918.

Li, W., Ishida, T., Tachibana, R., Almofti, M.R., Wang, X., Kiwada, H., 2004. Cell type-specific gene expression, mediated by TFL-3, a cationic liposomal vector, is controlled by a post-transcription process of delivered plasmid DNA. Int. J. Pharm. 276, 67–74.

Li, W., Ishida, T., Okada, Y., Oku, N., Kiwada, H., 2005. Increased gene expression by cationic liposomes (TFL-3) in lung metastases following intravenous injection. Biol. Pharm. Bull. 28, 701–706.

Lundstrom, K., Boulikas, T., 2003. Viral and non-viral vectors in gene therapy: technology development and clinical trials. Technol. Cancer Res. Treat. 2, 471–486.

Martinez, J., Patkaniowska, A., Urlaub, H., Luhrmann, R., Tuschl, T., 2002. Single-stranded antisense siRNAs guide target RNA cleavage in RNAi. Cell 110, 563–574.

Morrissey, D.V., Lockridge, J.A., Shaw, L., Blanchard, K., Jensen, K., Breen, W., Hartsough, K., Machemer, L., Radka, S., Jadhav, V., Vaish, N., Zinnen, S., Vargeese, C., Bowman, K., Shaffer, C.S., Jeffs, L.B., Judge, A., MacLachlan, I., Polisky, B., 2005. Potent and persistent in vivo anti-HBV activity of chemically modified siRNAs. Nat. Biotechnol. 23, 1002–1007.

Muratovska, A., Eccles, M.R., 2004. Conjugate for efficient delivery of short interfering RNA (siRNA) into mammalian cells. FEBS Lett. 558, 63–68.

Nguyen, L.T., Ishida, T., Ukitsu, S., Li, W., Tachibana, R., Kiwada, H., 2003. Culture time-dependent gene expression in isolated primary cultured rat hepatocytes by transfection with the cationic liposomal vector TFL-3. Biol. Pharm. Bull. 26, 880–885.

Nguyen, L.T., Ishida, T., Kiwada, H., 2005. Gene expression in primary cultured mouse hepatocytes with a cationic liposomal vector, TFL-3: comparison with rat hepatocytes. Biol. Pharm. Bull. 28, 1472–1475.

Nogawa, M., Yuasa, T., Kimura, S., Tanaka, M., Kuroda, J., Sato, K., Yokota, A., Segawa, H., Toda, Y., Kageyama, S., Yoshiki, T., Okada, Y., Maekawa, T., 2005. Intravesical administration of small interfering RNA targeting PLK-1 successfully prevents the growth of bladder cancer. J. Clin. Invest. 115, 978–985.

Paddison, P.J., Caudy, A.A., Hannon, G.J., 2002. Stable suppression of gene expression by RNAi in mammalian cells. Proc. Natl. Acad. Sci. U.S.A. 99, 1443–1448.

Ross, P.C., Hui, S.W., 1999. Lipoplex size is a major determinant of in vitro lipofection efficiency. Gene Ther. 6, 651–659.

Schiffelers, R.M., Ansari, A., Xu, J., Zhou, Q., Tang, Q., Storm, G., Molema, G., Lu, P.Y., Scaria, P.V., Woodle, M.C., 2004. Cancer siRNA therapy by tumor selective delivery with ligand-targeted sterically stabilized nanoparticle. Nucleic Acids Res. 32, e149.

Schwarz, D.S., Hutvagner, G., Haley, B., Zamore, P.D., 2002. Evidence that siRNAs function as guides, not primers, in the *Drosophila* and human RNAi pathways. Mol. Cell. 10, 537–548.

Simberg, D., Danino, D., Talmon, Y., Minsky, A., Ferrari, M.E., Wheeler, C.J., Barenholz, Y., 2001. Phase behavior, DNA ordering, and size instability of cationic lipoplexes. Relevance to optimal transfection activity. J. Biol. Chem. 276, 47453–47459.

Sioud, M., Sorensen, D.R., 2003. Cationic liposome-mediated delivery of siRNAs in adult mice. Biochem. Biophys. Res. Commun. 312, 1220–1225.

Sioud, M., Sorensen, D.R., 2004. Systemic delivery of synthetic siRNAs. Methods Mol. Biol. 252, 515–522.

Sorensen, D.R., Leirdal, M., Sioud, M., 2003. Gene silencing by systemic delivery of synthetic siRNAs in adult mice. J. Mol. Biol. 327, 761–766.

Spagnou, S., Miller, A.D., Keller, M., 2004. Lipidic carriers of siRNA: differences in the formulation, cellular uptake, and delivery with plasmid DNA. Biochemistry 43, 13348–13356.

Xu, Y., Zhang, H., Thormeyer, D., Larsson, O., Du, Q., Elmen, J., Wahlestedt, C., Liang, Z., 2003. Effective small interfering RNAs and phosphorothioate antisense DNAs have different preferences for target sites in the luciferase mRNAs. Biochem. Biophys. Res. Commun. 306, 712–717.

Xu, Y., Linde, A., Larsson, O., Thormeyer, D., Elmen, J., Wahlestedt, C., Liang, Z., 2004. Functional comparison of single- and double-stranded siRNAs in mammalian cells. Biochem. Biophys. Res. Commun. 316, 680–687.

Yano, J., Hirabayashi, K., Nakagawa, S., Yamaguchi, T., Nogawa, M., Kashimori, I., Naito, H., Kitagawa, H., Ishiyama, K., Ohgi, T., Irimura, T., 2004. Antitumor activity of small interfering RNA/cationic liposome complex in mouse models of cancer. Clin. Cancer Res. 10, 7721–7726.

Enhancement of Anticancer Activity in Antineovascular Therapy Is Based on the Intratumoral Distribution of the Active Targeting Carrier for Anticancer Drugs

Noriyuki MAEDA,[a,b] Souichiro MIYAZAWA,[a] Kosuke SHIMIZU,[a] Tomohiro ASAI,[a] Sei YONEZAWA,[a] Sadaya KITAZAWA,[b] Yukihiro NAMBA,[b] Hideo TSUKADA,[c] and Naoto OKU*[,a]

[a] *Department of Medical Biochemistry and COE Program in the 21st Century, School of Pharmaceutical Sciences, University of Shizuoka; 52–1 Yada, Suruga-ku, Shizuoka 422–8526, Japan:* [b] *Nippon Fine Chemical Co., Ltd.; 5–1–1 Umei, Takasago, Hyogo 676–0074, Japan: and* [c] *Central Research Laboratory, Hamamatsu Photonics K.K.; 5000 Hirakuchi, Hamamatsu 434–8601, Japan.*

Received April 17, 2006; accepted June 22, 2006; published online June 28, 2006

We previously observed the enhanced anticancer efficacy of anticancer drugs encapsulated in Ala-Pro-Arg-Pro-Gly-polyethyleneglycol-modified liposome (APRPG-PEG-Lip) in tumor-bearing mice, since APRPG peptide was used as an active targeting tool to angiogenic endothelium. This modality, antineovascular therapy (ANET), aims to eradicate tumor cells indirectly through damaging angiogenic vessels. In the present study, we examined the *in vivo* trafficking of APRPG-PEG-Lip labeled with [2-^{18}F]2-fluoro-2-deoxy-D-glucose ([2-^{18}F]FDG) by use of positron emission tomography (PET), and observed that the trafficking of this liposome was quite similar to that of non-targeted long-circulating liposome (PEG-Lip). Then, histochemical analysis of intratumoral distribution of both liposomes was performed by use of fluorescence-labeled liposomes. In contrast to *in vivo* trafficking, intratumoral distribution of both types of liposomes was quite different: APRPG-PEG-Lip was colocalized with angiogenic endothelial cells that were immunohistochemically stained for CD31, although PEG-Lip was localized around the angiogenic vessels. These results strongly suggest that intratumoral distribution of drug carrier is much more important for therapeutic efficacy than the total accumulation of the anticancer drug in the tumor, and that active delivery of anticancer drugs to angiogenic vessels is useful for cancer treatment.

Key words cancer antineovascular therapy; long-circulating liposome; angiogenesis; active targeting; positron emission tomography (PET)

Angiogenesis is critical for maintenance, proliferation and hematogenous metastasis of tumor.[1,2] Recently, various antiangiogenic therapeutic modalities have accomplished remarkable progress. We previously proposed cancer antineovascular therapy (ANET)[3,4]: Indirect tumor regression is achieved through damaging neovessel endothelial cells by anticancer drugs, since neovessel endothelial cells are growing cells and are susceptible to anticancer drugs like as tumor cells. For this purpose, we isolated APRPG peptide specifically bound to tumor angiogenic vasculature from phage-displayed peptide library, and observed that APRPG-modified liposomes accumulated in tumor tissue higher than unmodified one in tumor-bearing mice. In addition, the liposomes encapsulating adriamycin (ADM) strongly suppressed tumor growth.[3] ANET is expected to suppress both primary tumor and metastasis without acquiring drug resistance. In fact, ADM-resistant P388 tumor was susceptible to ADM encapsulated in APRPG-modified liposomes.[5] The therapy is also expected for a broad spectrum of cancers.

On the other hand, it is known that polyethyleneglycol (PEG)-coated liposomes have long-circulating characteristics through avoidance of uptake by reticuloendothelial system (RES) such as liver and spleen,[6,7] because PEG-coating protects liposomes from opsonization and attack of lipoproteins by their surface aqueous layers.[8] Furthermore, PEG-coated liposomes are expected to accumulate in tumor tissue through leaky vasculature of angiogenic vessels by enhanced permeability and retention (EPR) effect.[9,10]

Therefore, we synthesized APRPG peptide attached to PEG termini of PEG-disteaoylphosphatidylethanolamine (PEG-DSPE) to prepare angiogenesis-targeted liposomes with long circulating characteristic.[11] We previously observed that ADM-encapsulated liposomes modified with APRPG-PEG caused more efficient tumor growth suppression than ADM-encapsulated liposomes modified with PEG alone in Colon 26 NL-17 carcinoma (C26 NL-17)-bearing mice, despite not so much different accumulation of both liposomes in the tumor.[12] To clarify the advantage of angiogenesis-targeted long-circulating liposomes, we examined the *in vivo* trafficking of APRPG-PEG-modified liposomes as well as non-modified or PEG-modified ones in tumor-baring mice with positron emission tomography (PET) in the present study: The method is able to determine the real time liposomal trafficking non-invasively.[13] Furthermore we investigated the intratumoral distribution of liposomes modified with APRPG-PEG by use of fluorescence-labeled liposomes, and observed that differential local distribution between APRPG-PEG-modified liposomes and those modified with PEG alone.

MATERIALS AND METHODS

Materials APRPG-PEG-conjugated DSPE (APRPG-PEG-DSPE) and PEG-conjugated DSPE (PEG-DSPE) were prepared as described previously.[11] StearoylAPRPG was synthesized according to the previous method.[3] Distearoylphosphatidylcholine (DSPC) was the product of Nippon Fine Chemical Co. (Hyogo, Japan). Cholesterol was purchased from Sigma (St. Louis, MO, U.S.A.). All other reagents used were the analytical grades.

Preparation of Liposomes Liposomes were prepared for the PET analysis as follows: DSPC and cholesterol with

* To whom correspondence should be addressed. e-mail: oku@u-shizuoka-ken.ac.jp

© 2006 Pharmaceutical Society of Japan

APRPG-PEG-DSPE or PEG-DSPE (10:5:1 as a molar ratio; APRPG-PEG-Lip or PEG-Lip, respectively), or DSPC and cholesterol without PEG conjugates (10:5 as a molar ratio; cont-Lip) were dissolved in chloroform and methanol, dried under reduced pressure, and stored *in vacuo* for at least 1 h. After hydration of the thin lipid films with 1.0 ml of 0.9 M glucose, the resulting liposomal solution was mixed 2.0 ml of [2-^{18}F]2-fluoro-2-deoxy-D-glucose ([2-^{18}F]FDG) solution and freeze-thawed for three cycles by liquid nitrogen in order to encapsulate the positron emitter-containing chemical into the liposomes: The osmolarity in the liposomal solution was similar to that under physiological condition. Then, the liposomes were extruded thrice through a polycarbonate membrane filter (100-nm pore size), washed by centrifugation at 180000×g for 15 min after dilution with phosphate-buffered saline (PBS) to remove the untrapped [2-^{18}F]FDG, and finally resuspended in 1 ml of 0.3 M glucose.

To examine the intratumoral localization of liposomes in tumor syngrafts, liposomes were fluorescence-labeled with 1,1′-dioctadecyl-3,3,3′,3′-tetramethylindo-carbocyanine perchlorate ($DiIC_{18}$; Molecular Probes Inc., Eugene, OR, U.S.A.). DSPC, cholesterol and $DiIC_{18}$ with APRPG-PEG-DSPE or PEG-DSPE (20:10:1:2 as a molar ratio), or DSPC, cholesterol and $DiIC_{18}$ without PEG conjugates (20:10:1 as a molar ratio) were dissolved in chloroform and methanol, dried under reduced pressure, and stored *in vacuo* for at least 1 h. After hydration of the thin lipid film with 1.0 ml of 0.3 M glucose, the resulting liposomal solution was freeze-thawed for three cycles by liquid nitrogen. Then, the liposomes were extruded thrice through a polycarbonate membrane filter (100-nm pore size).

For therapeutic experiment, ADM-encapsulated liposomes were prepared by a modification of the remote-loading method as described previously,[12] and the encapsulation efficiency determined was more than 90% throughout the experiment. The concentration of ADM was determined by 484-nm absorbance.

PET Analysis of APRPG-PEG Modified Liposomes C26 NL-17 cells (1.0×10^6 cells/mouse) were injected subcutaneously into the posterior flank of 5-week-old BALB/c male mice (Japan SLC Inc., Shizuoka, Japan), and PET study was performed when the tumor size had become about 10 mm in diameter. Tumor-bearing mice weighing 23—26 g were injected into a tail vein with positron-labeled liposomes. The injected dose was 2 mmol as DSPC dosage, and about 0.5 MBq. The emission scan was started immediately after injection and performed for 120 min with an animal PET camera (Hamamatsu Photonics K.K., SHR-7700) having an effective slice aperture of 3.6 mm. Transmission scans were obtained by use of an 18.5 MBq ^{68}Ga/Ga ring source for attenuation correction before the liposomal injection. The radioactivity in the form of coincident gamma photons was measured and converted to Bq/cm^3 of tissue volume by calibration after correction for decay and attenuation. A time activity curve was obtained from the mean pixel radioactivity in the region of interest (ROI) of the PET images.

Histochemical Analysis of Liposomal Distribution in Tumor Syngrafts C26 NL-17 cells (1.0×10^6 cells/mouse) were inoculated as described above. $DiIC_{18}$-labeled liposomes were administered *via* a tail vein of C26 NL-17-bearing mice when the tumor sizes had reached about 10 mm. Two hours after the injection of liposomes, mice were sacrificed under anesthesia with diethyl ether, and the tumor was dissected. Solid tumors were embedded in optimal cutting temperature compound (Sakura Finetechnochemical Co., Ltd., Tokyo, Japan) and frozen at −80 °C. Five-micrometer tumor sections were prepared by using cryostatic microtome (HM 505E, Microm, Walldorf, Germany), mounted on MAS coated slides (MATSUNAMI GLASS Ind., Ltd., Japan), and air-dried for 1 h. The tissue sections were fixed in acetone for 10 min at room temperature, washed twice with PBS (5 min each time), and incubated with protein-blocking solution containing 1% bovine serum albumin in PBS for 10 min at room temperature. Then, the samples were incubated with an appropriately diluted (1 : 100) biotinylated anti-mouse CD31 rat monoclonal antibody (Becton Dickinson Lab., Franklin Lakes, NJ, U.S.A.) for 18 h at 4 °C. After the sections were rinsed three times (2 min each time) with PBS, they were incubated with streptavidin-FITC conjugates (Molecular Probes Inc., Eugene, OR, U.S.A.) for 30 min at room temperature in a humid chamber. Samples were washed twice with PBS (2 min each time). Finally, sections were counterstained and mounted with Perma Fluor Aqueous Mounting Medium (Thermo Shandon, Pittsburgh, PA, U.S.A.). These sections were fluorescently observed by using microscopic LSM system (Carl Zeiss Co., Ltd.): Endothelial cells were identified as green fluorescence and liposomes were detected as red.

Therapeutic Experiment C26 NL-17 cells (1.0×10^6 cells/mouse) were inoculated as described above. Liposomes encapsulating ADM or 0.3 M glucose solution were administered intravenously into C26 NL-17-bearing mice at day 11, 14, and 17 after the inoculation of tumor cells: The treatment was started when the tumor volumes became about 0.1 cm^3. The injected dose of ADM in each administration was 10 mg/kg (about 0.045 mmol/kg liposomal dose as DSPC in liposomal formulations). The size of the tumor and body weight of each mouse were monitored. Two bisecting diameters of each tumor were measured with slide calipers to determine the tumor volume and calculation was performed using the formula $0.4\times(a\times b^2)$, where a is the largest and b is the smallest diameter.

Statistical Analysis Differences in a group were evaluated by Student's t-test.

RESULTS

***In Vivo* Trafficking of [2-^{18}F]FDG-Labeled Liposomes Imaged by PET** We examined *in vivo* behavior of liposomes visually by use of PET. A PET study allows us to analyze real time distribution change of liposomes under non-invasive conditions. Liposomes prelabeled with [2-^{18}F]FDG were injected into C26 NL-17-bearing mice, and PET analysis was performed. PET images (Fig. 1a) and the time activity curves of liposomal ^{18}F (Fig. 2a) in the tumor indicated that APRPG-PEG-coated and PEG-modified liposomes highly accumulated in the tumor immediately after the injection, and this high accumulation was sustained for at least 120 min during PET scanning. The PET study also showed that APRPG-PEG-Lip and PEG-Lip tended to avoid RES trapping (Figs. 1b, c, Figs. 2b, c) consistent with previous observation.[13] In contrast to PEG-modified liposomes, cont-Lip tended to accumulate in the liver and spleen. These results

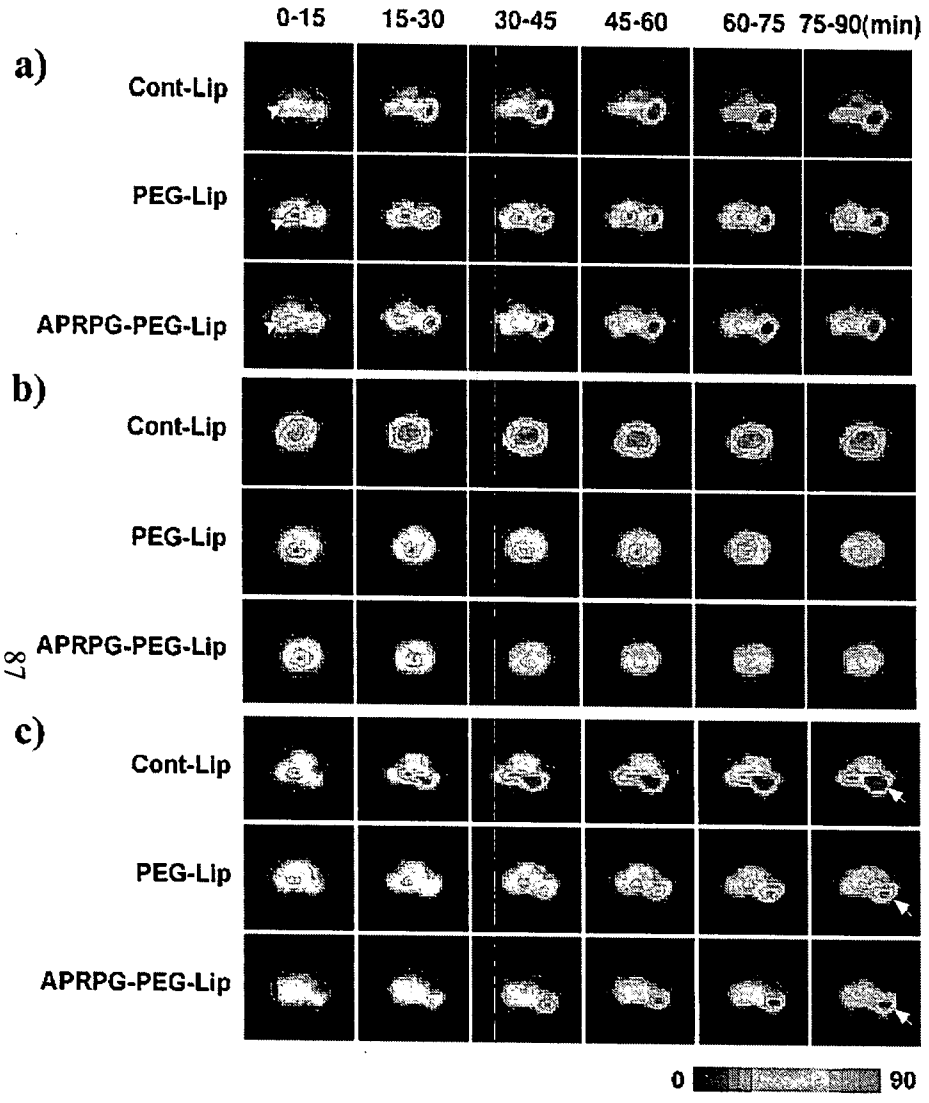

Fig. 1. PET Images of [2-^{18}F]FDG-Labeled Liposomal Distribution

Liposome composed of DSPC and cholesterol (upper panel), with DSPE-PEG (middle panel) or with DSPE-PEG-APRPG (lower panel) was prepared at a molar ratio of 10 : 5 : 1 in the presence of [2-^{18}F]FDG and extruded through 100-nm pores as described in Section 2. Gradation was corrected to be comparable in three groups. PET images show the accumulation of liposomes in the tumor (a), liver (b), or spleen (c) during every 15 min after injection. Coronal images of the tumor in each mouse are shown. Arrowheads indicate a location of the tumor. Arrows indicate that of the spleen. A separate experiment in the same procedure was performed and the similar results were obtained. Gradation bar indicates signal intensity.

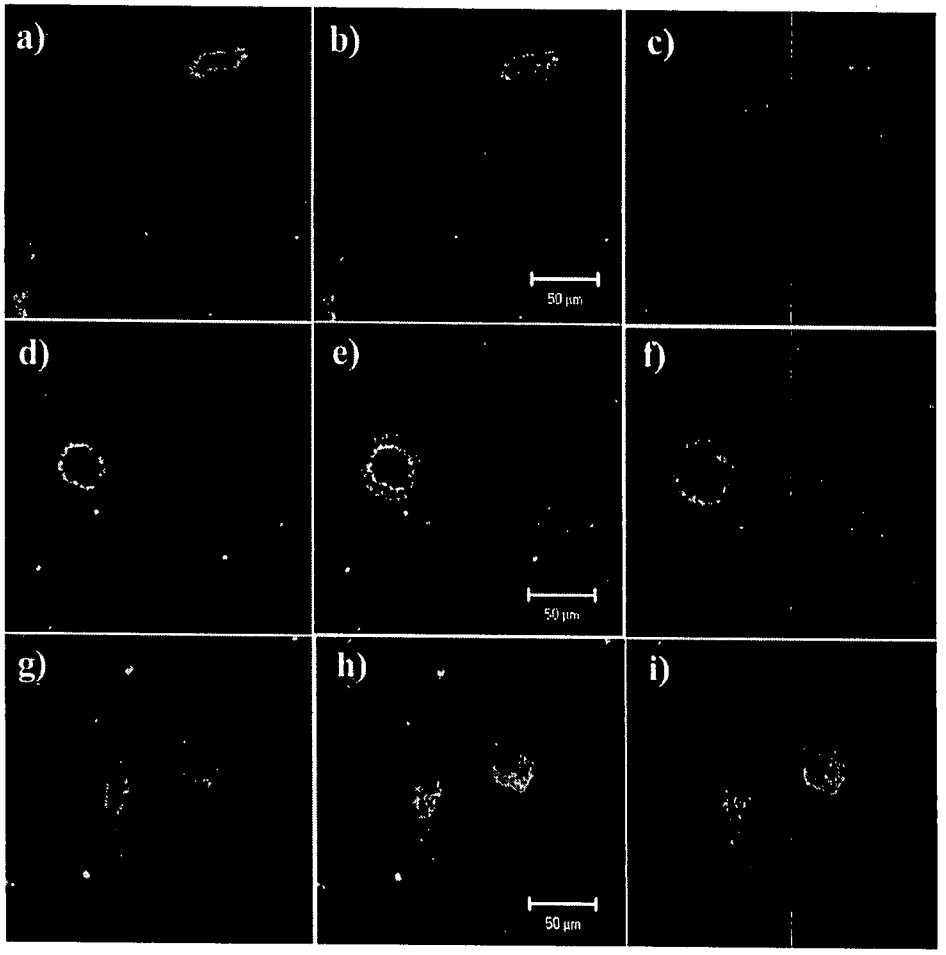

Fig. 3. Intratumoral Localization of DiIC$_{18}$-Labeled Liposomes after Injection

C26 NL-17-bearing mice were injected with Cont-Lip (a—c), PEG-Lip (d—f) or APRPG-PEG-Lip (g—i) labeled with DiIC$_{18}$ (c, f and i as red images) *via* tail vein on day 20 after tumor implantation. At 2 h after injection, each tumor was dissected and prepared for frozen-section. Micrographs derived from the image of CD31-staining vessels (a, d and g as green images). Panels b, e and h show the merged images of liposomal distribution and immunostaining for CD31, respectively. Yellow portions indicate localization of liposomes at the site of vascular endothelial cells. Separate experiments in the same procedure were performed and the similar results were obtained.

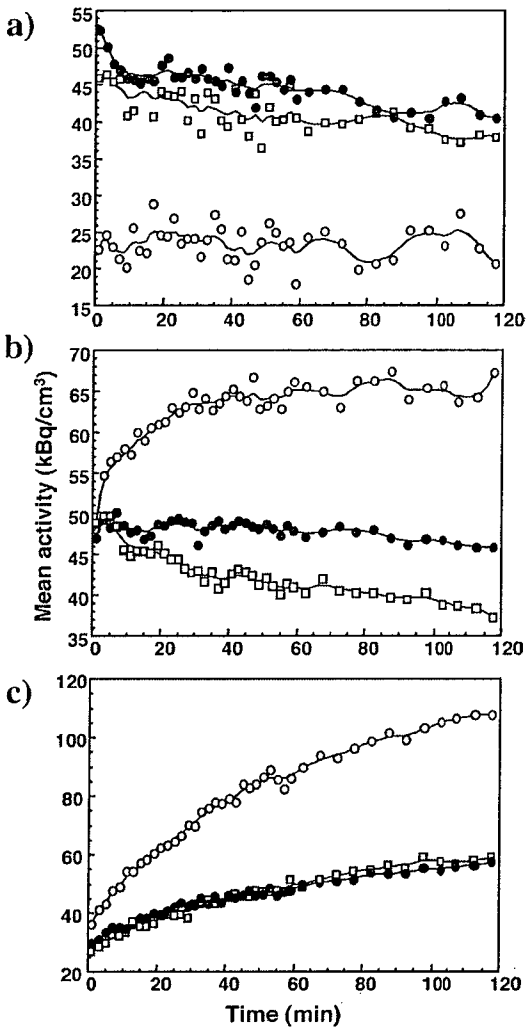

Fig. 2. Time-Dependent Accumulation of [2-^{18}F]FDG-Labeled Liposomes in Various Organs

Time–activity curves of ^{18}F in tumor (a), liver (b) and spleen (c) were obtained from the mean pixel radioactivity in ROI of the images shown in Fig. 1. C26 NL-17 carcinoma-bearing mice were injected with [2-^{18}F]FDG-labeled Cont-Lip (open circle), PEG-Lip (closed circle) or APRPG-PEG-Lip (open square).

were confirmed by the actual ^{18}F accumulation in the tumor, liver and spleen dissected from the mice after PET scanning (data not shown).

Intratumoral Distribution of APRPG-PEG-Modified Liposomes C26 NL-17-bearing mice were given a single i.v. dose of APRPG-PEG-Lip, PEG-Lip or Cont-Lip labeled with $DiIC_{18}$, and the mice were euthanized with diethylether anesthesia. Angiogenic endothelial cells in frozen sections of tumor organs were stained by immunohistochemical techniques and liposomal distribution in them was observed under confocal laser scanning microscopy. As shown in Figs. 3a—c, only a small amount of red fluorescence was observed, and some of them were surrounded with green fluorescence when cont-Lip was injected. On the contrary, red fluorescence was widely observed outside of green fluorescence in Figs. 3d—f, suggesting that PEG-Lip extravasated from tumor angiogenic vessels and accumulated in the tumor tissue. Interestingly, fluorescence of APRPG-PEG-Lip was colocalized with CD31-staining (Figs. 3g—i), suggesting that APRPG-PEG-Lip associated with angiogenic endothelial cells.

Table 1. Therapeutic Efficacy of APRPG-PEG-Modified Liposome Encapsulating ADM on Tumor-Bearing Mice

Treatment	Tumor volume (cm^3)	Growth inhibition (%)	Mean survival (d)
Control	3.28±0.52	—	50.3±6.0
APRPG-LipADM	1.38±0.69	57.8	55.5±7.8
PEG-LipADM	1.10±0.47	66.3	61.3±9.0
APRPG-PEG-LipADM	0.59±0.32[a)]	82.1	70.0±10.3[b)]

a) Significantly different from control ($p<0.001$), APRPG-LipADM ($p<0.05$) and PEG-LipADM ($p<0.05$). *b*) Significantly different from control ($p<0.001$) and APRPG-LipADM ($p<0.05$). C26 NL-17-bearing BALB/c mice ($n=6$) were injected i.v. with 0.3 M glucose (control), APRPG-LipADM, PEG-LipADM, or APRPG-PEG-LipADM for three times at day 11, 14 and 17 after the tumor implantation. Injected solutions of liposomal ADM were adjusted to 10 mg/kg as ADM concentration in each administration. The size change of the tumor at day 27 and the survival time of tumor-bearing mice are shown.

Therapeutic Efficacy of APRPG-PEG-Lip Encapsulating ADM Finally, therapeutic experiment was performed in a similar manner to that in a previous report[13] except that the effect of APRPG-modified non-pegylated liposomes was examined as well as that of pegylated liposomes at the present study: The liposomes encapsulating ADM (10 mg/kg as ADM in each administration) were injected thrice into C26 NL-17-bearing mice. As shown in Table 1, APRPG-PEG-LipADM suppressed tumor growth most efficiently compared with PEG-LipADM and APRPG-LipADM: The significant difference in tumor volume of APRPG-PEG-LipADM-treated group from that of the control ($p<0.001$), APRPG-LipADM-treated ($p<0.05$), and PEG-LipADM-treated group ($p<0.05$) was observed. Additionally, the results of body weight change indicated that liposomalization suppressed severe side effects of the drug in consistent with the previous results[11] (data not shown). Corresponding to the tumor growth suppression, treatment with APRPG-PEG-LipADM, elongated the survival time of the mice.

DISCUSSION

In general, treatment with anti-cancer drugs accompanies severe side effects, since they have the strong cytotoxicity against not only tumor cells but also normal growing cells. In order to prevent from severe side effects of these drugs, liposomes are useful tools for the carrier of these drugs. It is known that PEG-modified liposomes prevent from phagocytosis by macrophage and opsonization since these liposomes have water layer on liposomal surface.[14] The feature of long-circulation causes the liposomal accumulation in tumor tissues because angiogenic vasculature in tumor tissue is quite leaky and macromolecules are easily accumulate in the interstitial spaces of the tumor due to EPR effect.[8,9] Besides passive targeting, active targeting of pegylated liposomes has been widely studied: The distal end of PEG on liposomal surface is modified with various kinds of molecules (for example antibodies, Fab' fragments or other ligands) in order to enhance the affinity for targeted cell surface.[15] However, when these liposomes are targeted at tumor cells, passive accumulation of liposomes by EPR effect is prerequisite for active binding of the drug carrier to the target molecules. This uncertainty may affect targeting efficacy and subsequent therapeutic effect.

Correspondingly, we have developed a novel modality of

cancer treatment, antineovascular therapy, by use of angiogenic vasculature-targeting peptide, APRPG.[3,4] These 5-mer peptide-modified liposomes tend to accumulate to tumor tissue through specific binding to neovascular endothelial cells. Furthermore, APRPG-modified ADM-encapsulated liposomes significantly suppressed tumor growth.[3] When the endothelial cell surface molecules are targeted, extravasation of liposome from bloodstream to tumor parenchyma may not be required because angiogenic endothelial cells ordinarily border to bloodstream. We previously tried to endow APRPG-LipADM with long-circulating character for enhancing the targeting ability of the drug carrier to angiogenic vessels, and observed that APRPG-LipADM was quite effective for tumor growth suppression.[12] Since it is not clear that the mechanism of the enhanced therapeutic efficacy is based on the damage of angiogenic endothelial cells by ADM encapsulated in APRPG-PEG-Lip, we examined *in vivo* trafficking and intratumoral distribution of APRPG-PEG-Lip in the present study.

The results of PET study indicate that PEG-coated liposomes, despite conjugating with APRPG peptide, avoided to be trapped by RES such as liver and spleen, and tended to accumulate to tumor more than non-modified one. However, the *in vivo* behavior and tumor accumulation of APRPG-PEG-Lip was almost the same as that of PEG-Lip. Therefore, we examined the liposomal localization in tumor tissues by use of fluorescence-labeled liposomes. As shown in Fig. 3, PEG-Lip extravasated through angiogenic vasculature and accumulated in the interstitial space of tumor tissues due to EPR effect. On the contrary, APRPG-PEG-Lip associated to angiogenic endothelial cells due to active targeting by APRPG peptide attached to liposomal surface, although it is unclear whether these liposomes only bound to the endothelial cells or they were internalized. Since peptides containing some basic amino acids such as HIV Tat peptide are known to electrically interact with plasma membrane and to be internalized,[16] it is possible that APRPG-PEG-Lip similarly interacted with the cells. However, we believe that APRPG-PEG-Lip interacted through a certain molecule on the cell surface, since the presence of excess peptide inhibited the binding of APRPG-Lip to VEGF-stimulated endothelial cells.[3]

Concerning the difference in intratumoral distribution between PEG-Lip and APRPG-PEG-Lip, apparent therapeutic efficacy of APRPG-PEG-LipADM shown in Table 1 would be explained that the damaging of angiogenic endothelial cells is effective for tumor growth suppression. This evidence suggests the importance of accessibility of liposomal anticancer drugs to angiogenic endothelial cells on therapeutic efficacy, rather than the total accumulation amount of them in tumor tissue.

Recently, Schiffelers *et al.*[17] and Pastorino *et al.*[18] reported ANET in similar idea to that of the present study by using targeting peptide-modified long-circulating liposomes encapsulating ADM: RGD peptide which might bind to integrin $\alpha_v\beta_3$ on the angiogenic endothelial cells or NGR peptide which targeted aminopeptidase N, a marker of these cells, was used as targeting molecules, respectively. As targeting molecules, short peptide fragments are very useful and attractive because of their ease of identification and production without heavy immunogenicity.

In this study, we compared the characteristics between APRPG-PEG-Lip and PEG-Lip, and demonstrated therapeutic potential of APRPG-PEG-LipADM in cancer chemotherapy. We concluded that this efficacy was partly referred from the active targeting efficiency of APRPG-PEG-Lip. Additionally, APRPG-PEG-Lip keeps long-circulating property, which enhances the opportunity of liposomal binding to angiogenic endothelial cells. Consequently, it would be expected that APRPG-PEG-Lip could effectively deliver anticancer agents for anti-neovascular therapy, or anti-angiogenic agents for tumor dormancy therapy. Furthermore, it is considered that APRPG-PEG may be useful for human cancer treatment, since APRPG-PEG-Lip have affinity for VEGF-stimulated human umbilical vein endothelial cells.[13]

REFERENCES

1) Folkman J., D'Amore P. A., *Cell*, **87**, 1153—1155 (1996).
2) O'Reilly M. S., Holmgren L., Chen C., Folkman J., *Nat. Med.*, **2**, 689—692 (1996).
3) Oku N., Asai T., Watanabe K., Kuromi K., Nagatsuka M., Kurohane K., Kikkawa H., Ogino K., Tanaka M., Ishikawa D., Tsukada H., Momose M., Nakayama J., Taki T., *Oncogene*, **21**, 2662—2669 (2002).
4) Asai T., Shimizu K., Kondo M., Kuromi K., Watanabe K., Ogino K., Taki T., Shuto S., Matsuda A., Oku N., *FEBS Lett.*, **520**, 167—170 (2002).
5) Shimizu K., Asai T., Fuse C., Sadzuka Y., Sonobe T., Ogino K., Taki T., Tanaka T., Oku N., *Int. J. Pharm.*, **296**, 133—141 (2005).
6) Sakakibara T., Chen F. A., Kida H., Kunieda K., Cuenca R. E., Martin F. J., Bankert R. B., *Cancer Res.*, **56**, 3743—3746 (1996).
7) Lasic D. D., *Nature* (London), **380**, 561—562 (1996).
8) Auguste D. T., Prud'homme R. K., Ahl P. L., Meers P., Kohn J., *Biochim. Biophys. Acta*, **1616**, 184—195 (2003).
9) Maeda H., Wu J., Sawa T., Matsumura Y., Hori K., *J. Control. Release*, **65**, 271—284 (2000).
10) Muggia F. M., *Clin. Cancer Res.*, **5**, 7—8 (1999).
11) Maeda N., Takeuchi Y., Takada M., Namba Y., Oku N., *Bioorg. Med. Chem. Lett.*, **14**, 1015—1017 (2004).
12) Maeda N., Takeuchi Y., Takada M., Sadzuka Y., Namba Y., Oku N., *J. Control. Release*, **100**, 41—52 (2004).
13) Oku N., *Adv. Drug Deliv. Rev.*, **37**, 53—61 (1999).
14) Oku N., *Adv. Drug Deliv. Rev.*, **40**, 63—73 (1999).
15) Allen T. M., *Nat. Rev. Cancer*, **2**, 750—763 (2002).
16) Fittipaldi A., Giacca M., *Adv. Drug Deliv. Rev.*, **57**, 597—608 (2005).
17) Schiffelers R. M., Koning G. A., ten Hagen T. L., Fens M. H., Schraa A. J., Janssen A. P., Kok R. J., Molema G., Storm G., *J. Control. Release*, **91**, 115—122 (2003).
18) Pastorino F., Brignole C., Marimpietri D., Cilli M., Gambini C., Ribatti D., Longhi R., Allen T. M., Corti A., Ponzoni M., *Cancer Res.*, **63**, 7400—7409 (2003).

Identification of oligopeptides binding to peritoneal tumors of gastric cancer

Noriyuki Akita,[1] Fukuto Maruta,[1,6] Leonard W. Seymour,[3] David J. Kerr,[3] Alan L. Parker,[4] Tomohiro Asai,[5] Naoto Oku,[5] Jun Nakayama[2] and Shinichi Miyagawa[1]

Departments of [1]Surgery and [2]Pathology, Shinshu University School of Medicine, Matsumoto, Japan; [3]Department of Clinical Pharmacology, Oxford University Radcliffe Infirmary, Oxford; [4]BHF Glasgow Cardiovascular Research Center, University of Glasgow, Glasgow, UK; [5]Department of Medical Biochemistry, School of Pharmaceutical Sciences, University of Shizuoka, Shizuoka, Japan

(Received March 13, 2006/Revised June 16, 2006/Accepted June 28, 2006/Online publication August 28, 2006)

This is a report of *in vivo* intraperitoneal biopanning, and we successfully identified a novel peptide to target the multiple peritoneal tumors of gastric cancer. A phage display library was injected directly into the abdominal cavity of mice bearing peritoneal tumors of human gastric cancer, and phages associated with the tumors were subsequently reclaimed from isolated samples. The tumor-associated phages were amplified and the biopanning cycle was repeated five times to enrich for high affinity tumor-selective binding peptides. Finally, a tri-peptide motif, KLP, which showed homology with laminin 5 (a ligand for α3β1 integrin), was identified as a binding peptide for peritoneal tumors of gastric cancer. Phage clones displaying the sequence KLP showed 64-fold higher binding to peritoneal tumors than control phage and were preferentially distributed in tumors rather than in normal organs after intraperitoneal injection into mice. In addition, the KLP phages were more likely to bind to cancer cells in malignant ascites derived from a patient with recurrent gastric cancer. Synthesized peptide containing the motif KLP (SWKLPPS) also showed a strong binding activity to peritoneal tumors without cancer growth effect. Liposomes conjugated with SWKLPPS peptide appeared significantly more often in tumors than control liposomes after intraperitoneal injection into mice. Furthermore, modification of liposomes with SWKLPPS peptide enhanced the antitumor activity of adriamycin on gastric cancer cells. The peptide motif KLP seems a potential targeting ligand for the treatment of peritoneal metastasis of gastric cancer. (*Cancer Sci* 2006; 97: 1075–1081)

Gastric cancer is the second-most common cancer in the world. Approximately 700 000 patients a year die from gastric cancer worldwide.[1] Peritoneal metastasis is the predominant metastatic pattern in advanced gastric cancer[2,3] and the prognosis of patients with peritoneal metastasis of gastric cancer is poor. The median survival time of such patients has been reported to be 3–6 months[4] and a standard treatment for peritoneal metastasis of gastric cancer has not yet been established.[5]

A big obstacle to establishing effective therapies for peritoneal metastasis of gastric cancer is the countless localities, including invisible ones such as cancer cell clusters in malignant ascites. Therefore, the establishment of a methodology that could target individual peritoneal metastatic tumors would bring about a dramatic improvement in the therapeutic efficacy of treatments for peritoneal metastasis. Furthermore, identification of suitable ligands that associate uniquely with peritoneal tumors could enable the selective delivery of anticancer drugs to these tumors, thereby decreasing drug entry into non-target cells and potentially allowing eradication of disseminated tumor tissues.

Candidate targeting agents have been studied by several groups attempting to confer tumor tropism. The ligands that have been evaluated include a large number of antibodies, including fragments and single chain Fv molecules[6] and growth factors, such as fibroblast growth factor[7] and vascular endothelial growth factor.[8] However, this empiric approach to the identification of targeting ligands has recently been largely superseded by the use of library-based screening systems, which have been designed to allow iterative selection of high affinity ligands by repeated screening and enrichment of living libraries.[9]

In the current study, we used a phage panning technique *in vivo* to identify peptides that bind specifically to peritoneal metastatic tumors of gastric cancer. The peptide-presenting phage library used was based on a combinatorial library of random peptide heptamers fused to a minor coat protein (pIII) of the M13 phage and contains approximately 2.8×10^9 different sequences.[10] Panning with the library against peritoneal tumors *in vivo* permits the identification of binding peptide sequences by extrapolation from the corresponding DNA sequences of phages recovered from the tumor nodules.

This is a report of *in vivo* intraperitoneal biopanning, and we successfully identified peptides capable of binding to peritoneal metastatic tumors. In this strategy, phage libraries were injected directly into the abdominal cavity of mice bearing peritoneal metastatic tumors, and phages associated with the tumors were subsequently reclaimed from isolated samples. The tumor-associated phages were then amplified and the biopanning cycle was repeated five times to enrich for high affinity tumor-selective binding peptides. In addition, in order to confirm the feasibility of future applications of the identified peptides to clinical practice, the tumor-binding and anticancer activities of one of the peptides were assessed after incorporation into liposomes.

Materials and Methods

Animals. Athymic female BALB/c nu/nμ mice, 6–7 weeks of age, originated from the Central Institute for Experimental Animals (Kawasaki, Japan), and were purchased from CLEA Japan (Tokyo, Japan). The mice were maintained in cages in a laminar airflow cabinet under specific pathogen-free conditions and provided with free access to sterile food and water.

Cell lines and cell culture. AZ-P7a cells, a human gastric carcinoma cell line, were kindly supplied by Dr T. Yasoshima (First Department of Surgery, Sapporo Medical University School of Medicine, Sapporo, Japan). The AZ-P7a cell line was derived from the AZ-521 human gastric cancer cell line and was previously reported to show a high potential for peritoneal metastasis in nude mice.[11]

Huh-7 cells, a human hepatocellular carcinoma cell line, were obtained from the Japan Health Science Foundation (Tokyo, Japan). DLD-1 cells, a human colorectal adenocarcinoma cell

[6]To whom correspondence should be addressed.
E-mail: maruta@hsp.md.shinshu-u.ac.jp

Abbreviations: ADM, adriamycin; BSA, bovine serum albumin; FCS, fetal calf serum; KLP, Lys-Leu-Pro; LipADM, adriamycin encapsulated in control liposome; PBS, phosphate-buffered saline; p.f.u., plaque-forming units; SWK-LipADM, adriamycin encapsulated in liposomes modified with stearoyl SWKLPPS.

doi: 10.1111/j.1349-7006.2006.00291.x
© 2006 Japanese Cancer Association

line, were obtained from the Cell Resource Center for Biomedical Research Institute of Development, Aging and Cancer (Tohoku University, Sendai, Japan).

All cells were maintained in RPMI-1640 medium (Sigma, St Louis, MO) supplemented with 10% FCS, 10^5 IU/L penicillin and 100 mg/L streptomycin (Sigma) in a humidified atmosphere of 95% air and 5% CO_2 at 37°C. The cells were passaged and expanded by trypsinization of the cell monolayers followed by replating every 4 days.

Mouse model of peritoneal metastasis of human gastric cancer. For mouse inoculation, cells in log-phase growth were harvested by trypsinization, and a medium containing 10% FCS was added. The cells were washed three times with PBS, resuspended in PBS, then maintained at 4°C until inoculation into mice. After fasting for 24 h, BALB/c nu/nμ mice were inoculated intraperitoneally with samples containing 1×10^7 AZ-P7a cells in 0.5 mL PBS. After 3 weeks, the inoculated mice had developed peritoneal metastases, and histological examination confirmed that these disseminated tumors consisted of AZ-P7a gastric cancer cells.

***In vivo* biopanning in mice with peritoneal metastases.** *In vivo* biopanning was carried out using the above-described mouse model of peritoneal metastasis. Three weeks after the inoculation of AZ-P7a human gastric cancer cells, the mice were anesthetized with diethyl ether and injected intraperitoneally with 2×10^{11} p.f.u. of the phage library (Ph.D.-7 M13 heptapeptide phage display peptide library kit; New England BioLabs, Beverly, MA) suspended in 1 mL of PBS. Twenty minutes after injection, the mice were killed and a few peritoneal metastatic tumor nodules were harvested from each mouse.

The harvested nodules were washed four times with PBS containing 0.5% Tween-20 (polyoxyethylene (20) sorbitan monolaurate; Kanto Chemical, Tokyo, Japan) to eliminate any unbound phages, then weighed, minced and homogenized in 5 mL PBS containing 1% protease inhibitor cocktail (Sigma) using a motor-driven Teflon-on-glass homogenizer. The homogenate was centrifuged at 450*g*. for 5 min (GS-15R; Beckman, Palo Alto, CA) and the supernatant was removed without disturbing the tissue pellet. The pellet was suspended in 5 mL of an acidic solution (0.2 M glycine-HCl, pH 2.2) for 3 min before being centrifuged at 450*g*. for 5 min to remove any weakly bound phages.[10] The remaining pellet (containing tightly bound phages) was neutralized by adding 750 μL of 1 M Tris-HCl (pH 9.1), then resuspended in 3 mL of PBS containing 0.5% Tween-20. The number of eluted phages was estimated by titering a small proportion on agar plates containing *Escherichia coli* strain ER2738 supplemented with 5-bromo-4-chloro-3-indolyl-beta-D-galactopyranoside (Wako, Osaka, Japan) and isopropyl beta-D-thiogalactopyranoside (Wako). The remaining phages were amplified by early log phase culture of ER2738 for 5 h at 37°C with vigorous shaking (150 r.p.m). The amplified phages were isolated from the resulting culture according to the manufacturer's recommended protocol, concentrated, titered and used for subsequent rounds of biopanning. In total, five consecutive rounds of biopanning were carried out in triplicate.

Isolation and sequencing of phage DNA. After each round of biopanning, individual phage clones were isolated from each replicate and their total DNA was isolated according to the recommended protocol of the sequencing kit manufacturer (Applied Biosystems, Foster, CA). The resulting DNA was used for sequencing analysis with –96 primer together with a BigDye terminator v3.0 cycle sequencing kit (Applied Biosystems). The DNA sequences were determined using an ABI PRISM 3100 Genetic Analyzer (Applied Biosystems).

Searches for human proteins mimicked by the selected peptide motifs were carried out using online databases available through the National Center for Biotechnology Information website (http:http://www.ncbi.nlm.nih.gov/BLAST/).

Evaluation of the binding activities of each selected phage to peritoneal metastases of gastric cancer. After five rounds of biopanning, some phage clones were identified as showing substantial binding to peritoneal metastases. The binding activity of individual phage clones was determined as follows. AZ-P7a human gastric cancer cells were inoculated intraperitoneally into nude mice. After 3 weeks, the mice were anesthetized and injected intraperitoneally with 2×10^{11} p.f.u. of each selected phage clone suspended in 1 mL of PBS. Twenty minutes after injection, the mice were killed and a few peritoneal metastatic tumor nodules in addition to normal organs (liver, stomach and spleen) were harvested from each mouse. Samples obtained from the tumors and normal organs were weighed, washed with PBS and homogenized. Phages were quantified by titering multiple dilutions of the homogenate, as described above. A phage clone displaying no oligopeptide insert (insertless) was used as a negative control. The results were expressed as p.f.u./g tissue.

From the results of the above-described experiments, KLP-containing motifs (SWKLPPS and QPLLKLP) were selected as the most promising consensus sequences and studied in more depth.

Immunohistochemistry. Samples from tumors and normal organs were fixed in buffered formalin, embedded in paraffin, sectioned and mounted on slides. For phage immunolocalization, a rabbit anti-fd bacteriophage antibody (Sigma) was used at 1:400 dilution. Horseradish peroxidase-conjugated swine antirabbit immunoglobulins (DAKO, Carpinteria, CA) were used as the secondary antibodies at 1:50 dilution. Positive signals were revealed by the addition of diaminobenzidine tetrahydrochloride.

Measurement of binding of selected phages to human cancer cell lines *in vitro*. The binding activities of selected phage clone to AZ-P7a (human gastric carcinoma), DLD-1 (human colorectal carcinoma) and Huh-7 (human hepatocellular carcinoma) cells were determined in six-well plates.

The cells were acclimatized at 4°C for 30 min, then washed briefly with PBS before the addition to each well of 5×10^7 p.f.u. of the selected phage clone diluted into 1 mL of RPMI-1640 medium containing 1% BSA (Sigma). The phages were allowed to bind to the cells for 1 h at 4°C with gentle agitation. The media containing unbound phages were discarded, and the cells were then washed four times in PBS containing 1% BSA, before 1 mL of acidic solution (0.2 M glycine-HCl, pH 2.2) was added for 5 min. The samples were then neutralized by adding 150 μL of 1 M Tris-HCl (pH 9.1), and the cell-associated phages were recovered by lysing the cells in 1 mL/well of 10 mM Tris-HCl (pH 8.0) containing 1 mM EDTA on ice for 1 h.

The recovery was determined by plaque infection assays of multiple dilutions of the eluted phages on bacterial lawns grown overnight on agar plates containing 5-bromo-4-chloro-3-indolyl-beta-D-galactopyranoside and isopropyl beta-D-thiogalactopyranoside at 37°C.

Competitive inhibitory effects of synthesized peptides on phage accumulation *in vitro* and *in vivo*. The inhibitory effects of the synthesized peptides on phage accumulation were examined. AZ-P7a cells were preincubated with 0.1 μM, 1 μM or 10 μM of the SWKLPPS peptide or QPLLKLP peptide (synthesized by SIGMA Genosys Japan, Ishikari, Japan) for 30 min at 4°C, and then 5×10^8 p.f.u. of the selected phage diluted in 1 mL RPMI containing 1% BSA was added. The phages were allowed to bind to the cells for 1 h at 4°C with gentle agitation. Media containing unbound phages were discarded, and the cells were then washed four times for 5 min each in PBS containing 1% BSA, before the cell-associated phages were recovered by lysing the cells in 1 mL/well of 30 mM Tris-HCl (pH 8.0) containing 10 mM EDTA on ice for 1 h. The number of phages recovered was determined by titering multiple dilutions of the eluted phages as described above. The same experiment was repeated using an irrelevant heptapeptide (TTPRDAY) as a control.

doi: 10.1111/j.1349-7006.2006.00291.x
© 2006 Japanese Cancer Association

The selected phage clone (2×10^{11} p.f.u.) and 10 μM or 1 mM of each synthesized peptide were co-injected intraperitoneally into the model mice with peritoneal metastases. The mice were anesthetized and killed 20 min after injection. The peritoneal metastatic tumor nodules were harvested, weighed, washed with PBS and homogenized. The tumor-associated phages were quantified by titering multiple dilutions of the homogenate, as described above.

Evaluation of the mitogenicity of the SWKLPPS peptide in AZ-P7a cells. AZ-P7a cells were plated in 96-well plates at 5×10^3 cells/well and incubated at 37°C in RPMI medium containing 10% FCS in either the presence or absence of 1 μM, 10 μM or 100 μM of the SWKLPPS peptide. After 24, 48, 72 and 96 h, the viability of the AZ-P7a cells was assessed using the MTS assay, as described previously.[12] Media were replaced with 120 μL of FCS-free RPMI containing 20 μL of CellTiter 96 AQueous One solution reagent (Promega, Madison, WI), and the culture plates were incubated at 37°C for 2 h. Next, 100 μL of the medium was transferred to a new 96-well plate and the quantity of the formazan product present was determined by measuring the absorbance at 490 nm using a microplate autoreader (Molecular Devices, Sunnyvale, CA).

Binding of SWKLPPS-conjugated phages to floating cells in malignant ascites derived from a patient with advanced gastric cancer. A 63-year-old male patient diagnosed with advanced gastric cancer had previously been treated by total gastrectomy and systemic chemotherapy. He was admitted to Shinshu University Hospital (Matsumoto, Japan) due to anorexia and severe abdominal distension. Therefore, an abdominal paracentesis was carried out to remove the ascites as a palliative treatment for his symptoms, and gastric cancer cells were cytologically proven to be present in the ascites. A part of the ascites was used for this study. Written informed consent was obtained from the patient prior to the study.

The collected ascites were centrifuged at 250*g*. for 5 min and the supernatant was removed without disturbing the pellet. The pellet was suspended in 30 mL of PBS and centrifuged at 250*g*. for 5 min before the supernatant was removed. This procedure was then repeated. The final pellet was suspended in 30 mL PBS and transferred to a 6-well plate (3 mL/well). After acclimatization of the cells at 4°C for 20 min, 5×10^8 p.f.u. of SWKLPPS phage or insertless control phage was added to each well of the plate. The phages were allowed to bind to the cells for 30 min at 4°C with gentle agitation. Then, the fluid was collected from each well, centrifuged at 250*g*. for 5 min and the supernatant was removed. After this procedure was repeated, the pellet was suspended in 2 mL of PBS. The number of phages binding to cells was determined by titering as described above.

Accumulation of SWKLPPS-conjugated liposomes in tumors of mice with peritoneal metastases. Distearoylphosphatidylcholine (Nippon Fine Chemical, Osaka, Japan), cholesterol (Sigma) and the stearoyl 7 mer peptide SWKLPPS (molar ratio of 10:5:1) or distearoylphosphatidylcholine and cholesterol without a peptide conjugate (molar ratio of 10:5) were dissolved in chloroform, dried under reduced pressure and stored *in vacuo* for at least 1 h. Liposomes were prepared by rehydration of the thin lipid film with 0.3 M glucose then subjected to three cycles of freezing and thawing using liquid nitrogen. Next, the liposomes were sized by extruding them three times through a polycarbonate membrane filter with 100 nm pores. For a biodistribution study, a trace amount of [1α,2α(*n*)-^{3}H] cholesterol oleoyl ether (Amersham Pharmacia, Buckinghamshire, UK) was added to the initial solution.

Mice with peritoneal metastases were prepared as described above. After 2 weeks, the mice were anesthetized and injected with radiolabeled liposomes containing [1α,2α(*n*)-^{3}H] cholesterol oleoyl ether intraperitoneally. Twenty-four hours after the injection, the mice were killed under diethyl ether anesthesia. The blood was collected from the carotid artery and centrifuged (600*g* for 5 min) to obtain the plasma. After the mice had been bled, the tumors and normal organs (stomach, liver, spleen, kidney, lung and heart) were removed, washed with saline and weighed. The radioactivity in each sample was determined with a liquid scintillation counter (LSC-3100; Aloka, Tokyo, Japan). The distribution data were presented as the percentage dose/100 mg wet tissue or the percentage dose/100 μL plasma.

Evaluation of anticancer activity of ADM-encapsulated liposomes modified with SWKLPPS. ADM-encapsulated liposomes were prepared by a modification of the remote-loading method as described previously.[13] The liposomal size and composition were the same as the accumulation study of liposomes. AZ-P7a cells were plated on a 96-well plate (5×10^3 cells/well in RPMI containing 10% FCS) and cultured in a CO_2 incubator at 37°C for 24 h. Next, 20 μL LipADM or SWK-LipADM was added to each well and allowed to bind to the cells for 30 min at 37°C. Then the mediums were changed to RPMI containing 10% FCS and the cells were cultured for a further 24 h. This experiment was repeated at the ADM concentration of 0.3, 1, 3, 10, 30 and 100 mg/mL. Cell proliferation assay was carried out as follows: 10 μL of TetraColor One reagent containing tetrazolium monosodium salt (Seikagaku, Tokyo, Japan) was added to each well; cells were incubated for 3 h; and absorbance at 450 nm was measured with a reference wavelength at 630 nm in the microplate reader.

Statistics. The results are represented as the mean ± standard deviation of the data from three independent experiments. The significance of differences was evaluated using Student's *t*-test or the Mann–Whitney U-test. The level of significance was set at $P < 0.05$.

Approval for this study was obtained prior to experimentation from the ethics committee of Shinshu University, and all animal procedures were carried out in compliance with the Guidelines for the Care and Use of Laboratory Animals in Shinshu University.

Results

Iteration of consensus oligopeptide sequence binding to peritoneal metastases. Five consecutive rounds of biopanning were carried out in mice with peritoneal metastases derived from human gastric cancer cells. The phage recovery from each round increased with the number of biopanning passages, except for the third round. After five rounds of selection, 14-fold more phages were recovered from peritoneal nodules compared to using the native phage library.

After each round of biopanning, individual phage plaques were picked up. Their DNA was isolated and sequenced, and the corresponding amino acid sequences of the inserts were deduced. After the first and second rounds of biopanning, the tumor-derived sequences displayed no distinguishable homology (data not shown). However, the tumor-derived sequences from the third, fourth and fifth rounds displayed some consensus motifs, and these were selected as candidate peptides that can bind to peritoneal metastases of gastric cancer. After the fifth round of biopanning, 90–100 phage plaques were picked up from each replicate, and their DNA was sequenced. Next, we compared the relative frequencies of every tri-peptide motif in each replicate. Tri-peptide motifs with a frequency of 2.5% or more in the fifth round were selected as candidate binding peptides. The motif frequencies were calculated as the prevalence of each motif-containing peptide divided by the total number of isolated peptides. KLP was the most frequently encountered tri-peptide (3.7%), followed by Prp-Pro-Leu (PPL; 3.3%), Ile-Pro-Pro (IPP; 3.3%), Ala-Asn-Pro (ANP; 2.9%), Ser-Pro-Thr (SPT; 2.9%) and Ala-Pro-Leu (APL; 2.8%).

To determine which motif was the best binding peptide, the binding activities of selected phage clones expressing the candidate oligopeptides were assessed *in vivo* as described above. The phage

© 2006 Japanese Cancer Association

clone expressing SWKLPPS showed the highest binding, with the recovery of 64-fold more phages compared with the insertless phage (control) (Fig. 1). Similarly, QPLLKLP showed a 43-fold higher recovery than the insertless phage. Therefore, the clones showing the best and second-best recoveries (SWKLPPS and QPLLKLP, respectively) both included the KLP motif. Accordingly, the KLP motif was selected as the most promising motif for binding to peritoneal metastases of gastric cancer.

Heptapeptides containing the consensus motif were analyzed using BLAST (National Center for Biotechnology Information) to search for similarity to known human peptides. Interestingly, KLP showed homology with laminin 5, which was reported to be a ligand for $\alpha 3\beta 1$ integrin.

Distribution of the selected phage in the mouse model of peritoneal metastasis. The phage clone displaying the sequence SWKLPPS was injected intraperitoneally into the model mice with peritoneal metastases. The phage accumulation in the tumors and organs was quantified by titering. The mean accumulation of the SWKLPPS phage in normal organs was less than 30% of that in tumors (Fig. 2a).

Immunohistochemistry was used to characterize the distribution of phage clones expressing the SWKLPPS peptide in the model mice with peritoneal metastases. The SWKLPPS phage showed strong binding to the tumor nodules (Fig. 2b,c), but only a low signal in normal organs such as the stomach, liver and spleen (Fig. 2e–g). Interestingly, the SWKLPPS phage appeared to be on the inside of the tumor nodules in addition to the surface, suggesting a possibility of penetration of the phage into the tumor nodules. However, the insertless phage only showed low signals in both tumors (Fig. 2d) and normal organs.

Binding activities of SWKLPPS-conjugated phages to human cancer cell lines. The binding activities of the phage clone expressing the SWKLPPS peptides was evaluated on confluent cultures of DLD-1 or Huh-7 cells, in comparison with AZ-P7a cells. The phages showed the greatest recovery from AZ-P7a cells. The recovery of the SWKLPPS phage from AZ-P7a cells was 1.3- and 13.9-fold higher than those from DLD-1 and Huh-7 cells, respectively. The similar recoveries of the SWKLPPS phage from AZ-P7a and DLD-1 can be explained by the supposition that the receptors for SWKLPPS might be similarly expressed in DLD-1 and AZ-P7a cells. However, the SWKLPPS phage bound to AZ-P7a cells 3-fold more strongly than the control phage in this *in vitro* experiment.

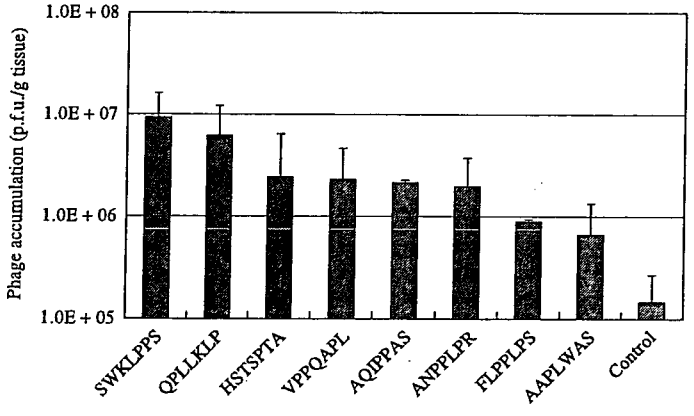

Fig. 1. *In vivo* binding activities of selected phage clones expressing the candidate peptides for binding to peritoneal tumors of gastric cancer. Each selected phage clone expressing the candidate peptides was injected intraperitoneally into model mice. The mice were killed 20 min after injection. Peritoneal tumor nodules were harvested from each mouse and homogenized, and the phages accumulated in the nodules were quantified by titering multiple dilutions of the homogenate. The results are expressed as p.f.u./g tissue, and a phage clone displaying no oligopeptide insert was used as a control.

Competitive inhibitory effects of synthesized peptides on phage accumulation *in vitro* and *in vivo*. To confirm the capacity of the synthesized peptides to accumulate in tumors, AZ-P7a cells were pre-incubated with 0.1, 1 or 10 μM of the SWKLPPS or QPLLKLP peptide before the addition of 5×10^8 p.f.u. of the selected phages. The inhibitory effects of the synthesized peptides on phage accumulation were examined by titering the phages bound to cancer cells. It was found that pre-incubation of cells with the SWKLPPS peptide caused 66% inhibition of the binding activity of the SWKLPPS phage to these cells (Fig. 3a). In addition, the binding of SWKLPPS phage was also inhibited by the addition of QPLLKLP peptide, indicating that the KLP motif played an important role in binding to the cancer cells in both SWKLPPS and QPLLKLP.

These inhibitory effects of the SWKLPPS peptide were also confirmed in an *in vivo* experiment using the model mice with peritoneal metastases (Fig. 3b). Similar to the *in vitro* experiment, the binding of SWKLPPS phage to peritoneal tumor was inhibited by co-injection of both of SWKLPPS and QPLLKLP peptides.

Assessment of the possible mitogenicity of the selected peptide. The possibility that the SWKLPPS peptide might play a role in cancer cell growth (promotion or inhibition) was evaluated using the MTS assay. The presence of the SWKLPPS peptide had no discernible effect on cell growth (Fig. 4).

Binding of the SWKLPPS phage to floating cells in malignant ascites from a patient with gastric cancer. We carried out an *ex vivo* experiment investigating SWKLPPS phage binding to floating cells in malignant ascites from a patient with gastric cancer. The SWKLPPS phage or insertless phage was co-incubated with malignant ascites from the patient, and the number of phages bound to the cells in the ascites was examined by phage-titering. The results revealed that the SWKLPPS phage bound to cells significantly more than control phage (Fig. 5).

Tumor binding and anticancer activities of SWKLPPS-conjugated liposomes in tumors. The accumulation of SWKLPPS-conjugated liposomes in tumors of mice with peritoneal metastasis of gastric cancer after intraperitoneal injection was examined. SWKLPPS-conjugated liposomes accumulated in the tumors significantly more than control liposomes (Fig. 6). On the contrary, significantly less SWKLPPS-conjugated liposomes appeared in the liver and kidney than control liposomes. In addition, we evaluated the anticancer activity of adriamycin-encapsulated liposomes modified with SWKLPPS (SWK-LipADM), using cell proliferation assay *in vitro*. SWK-LipADM showed more efficient anticancer activity than control (LipADM) (Fig. 7).

Discussion

In the present study, we used a phage display library to identify peptide sequences capable of binding to peritoneal metastases of gastric cancer, with the aim of enabling the use of ligands for delivery of agents to such peritoneal metastases. After five rounds of selection, the consensus sequence KLP was identified and the KLP-containing peptides were examined in more depth. Sequence analysis revealed that KLP showed homology with laminin 5. Laminin 5 has been reported to serve as a high-affinity ligand for $\alpha 3\beta 1$ integrin.[14,15] Immunohistochemical analysis of specimens of gastric cancer resected from more than 100 patients revealed that the expression of $\alpha 3\beta 1$ integrin was positively correlated with the occurrence of peritoneal and liver metastases and with increased invasiveness of the tumors.[16] AZ-P7a cells, the human gastric cancer cell line used in this study, possess a high potential for peritoneal dissemination, and were reported to express a significantly higher level of $\alpha 3$ integrins than AZ-521 cells, from which the AZ-P7a cell line was derived.[11] Taken together, there is a possibility that $\alpha 3\beta 1$ integrin is one candidate for the binding site of the KLP peptide.

doi: 10.1111/j.1349-7006.2006.00291.x
© 2006 Japanese Cancer Association

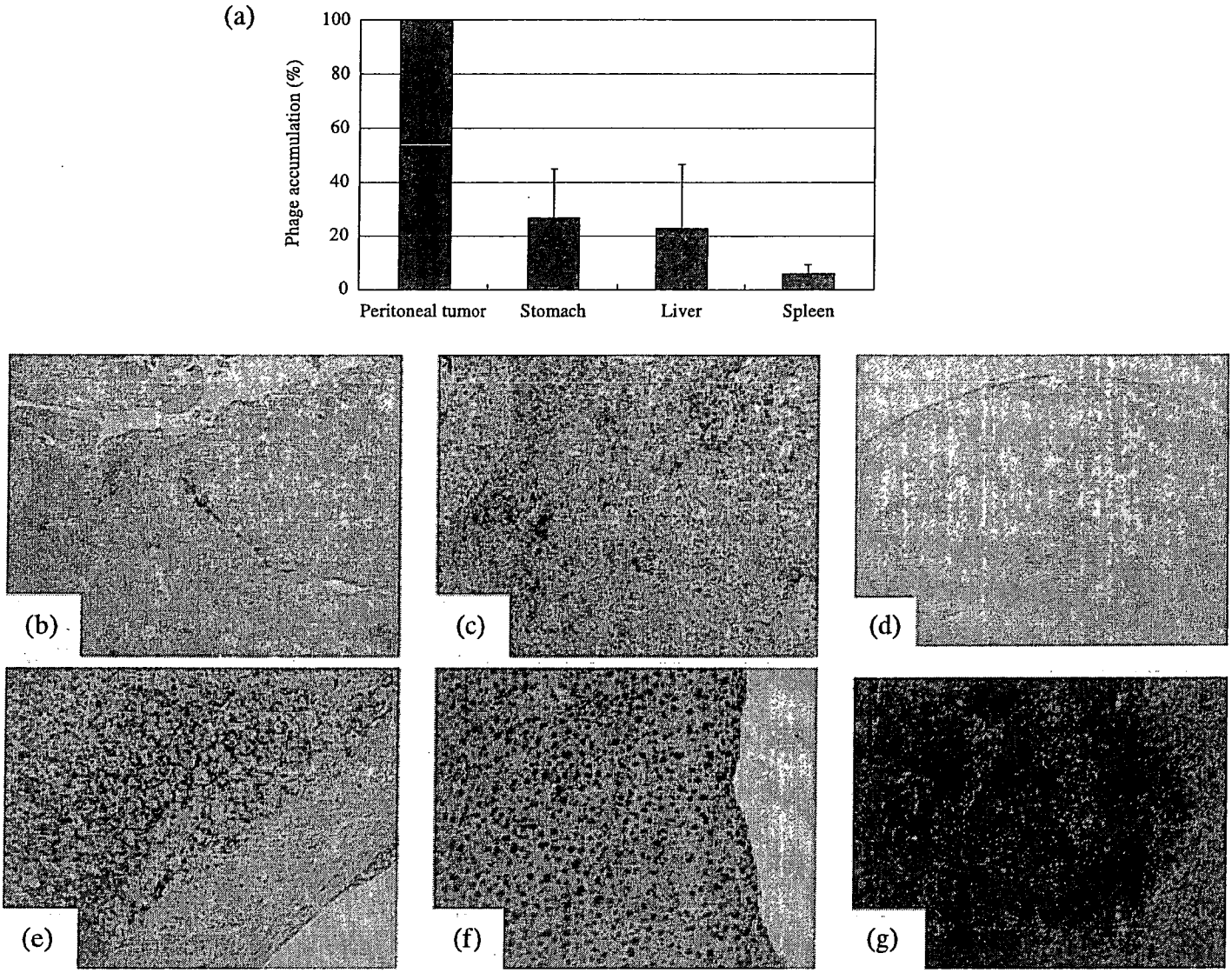

Fig. 2. Distribution of selected phage clones in model mice with peritoneal metastases. Twenty minutes after intraperitoneal injection of phage clones displaying the SWKLPPS sequence into model mice with peritoneal metastases, samples from the peritoneal tumors, normal stomach, liver and spleen were obtained. The distributions of the phages in the tumors and organs were quantified by titering and expressed as percentages of the accumulation in each organ compared to that in tumors (a). Simultaneously, the phage distributions were evaluated by immunohistochemistry (b–g). Phage accumulation is revealed by brown dots in each figure. (b, c) SWKLPPS phages in a tumor (magnification: ×40 and ×100, respectively). (d) Control phages in a tumor (magnfication: ×40). (e–g) SWKLPPS phages in the stomach, liver and spleen, respectively (magnification: ×100).

Phage display libraries have shown particular promise for elucidating receptor-binding peptides, and have recently been used *in vitro* to identify receptor-binding mimetics of fibroblast growth factor[17] and vascular endothelial growth factor.[18] However, the major strength of phage libraries is their suitability for application *in vivo* to enable the identification of ligands capable of targeting specific cells and organs.[19,20] By carrying out the selection procedure *in vivo*, the identified ligands are likely to be active under physiological conditions and their receptors will be accessible with an appropriate route of administration. In particular, this avoids the selection of ligands that bind to receptors that are inaccessible in the polarized *in vivo* cellular anatomy. Targeting systems that work well *in vitro* but fail *in vivo* due to polarization or inaccessibility of the receptors is well known.[21] Therefore, it was important that SWKLPPS was identified as a peptide that bound to peritoneal tumors in an *in vivo* experiment. Our study showed that the binding efficiency of the SWKLPPS phage to peritoneal tumors was greater *in vivo* than *in vitro* (64- *versus* 3-fold higher than the control, respectively). One possible explanation for this difference is that SWKLPPS might bind to some receptors predominantly activated *in vivo*, and works better *in vivo* than *in vitro*.

As described above, *in vivo* biopanning procedures using phage display libraries have been used to identify binding peptides for certain organs and tumors.[19–22] and in the majority of these studies, the phage libraries were injected intravenously. In contrast, intraperitoneal *in vivo* biopanning was used in our study, and we isolated the tumor-binding peptide SWKLPPS. Compared to intravenous injection, the intraperitoneal approach is clearly more useful for identifying peptides that bind to peritoneal metastases, as a larger number of phages reach the peritoneal tumors after intraperitoneal injection than after intravenous injection. Intraperitoneally injected agents, including phages, reach the tumor directly, whereas a considerable amount of intravenously injected agent is trapped by the reticuloendothelial system, such as the liver and spleen.

Another important advantage of intraperitoneal injection in animals bearing peritoneal metastases of human cancer is that the injected phages bind directly to the human cancer tissue

© 2006 Japanese Cancer Association

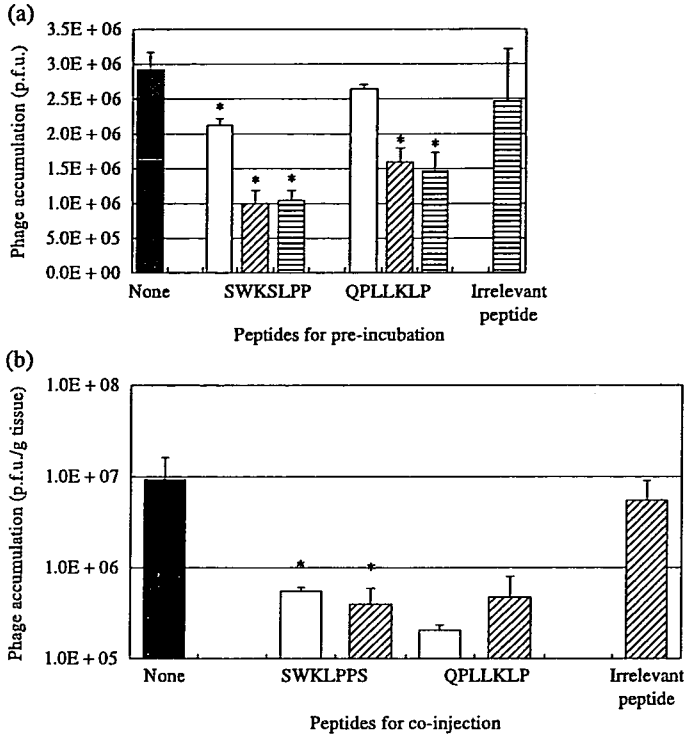

Fig. 3. Competitive inhibition of synthesized peptides against phage accumulation. AZ-P7a cells were pre-incubated with 0.1 (□), 1 (▨) or 10 μM (▤) of the SWKLPPS or QPLLKLP peptide for 30 min at 4°C, followed by the addition of 5×10^8 p.f.u. of the SWKLPPS phage *in vitro*. The inhibitory effects of the synthesized peptides on phage accumulation were examined by titering the phages bound to the cells (a). Similarly, the SWKLPPS phage (2×10^{11} p.f.u.) and 10 μM (□) or 1 mM (▨) of each synthesized peptide were co-injected intraperitoneally into model mice with peritoneal metastases. The mice were killed 20 min after injection. Peritoneal tumor nodules were harvested, and the phages accumulated in the tumors were quantified by titering to confirm the *in vivo* inhibitory effects of the synthesized peptides on phage accumulation (b). An irrelevant heptapeptide (TTPRDAY, 10 μM *in vitro* and 1 mM *in vivo*) was used as a control. $^*P < 0.05$ compared to the control.

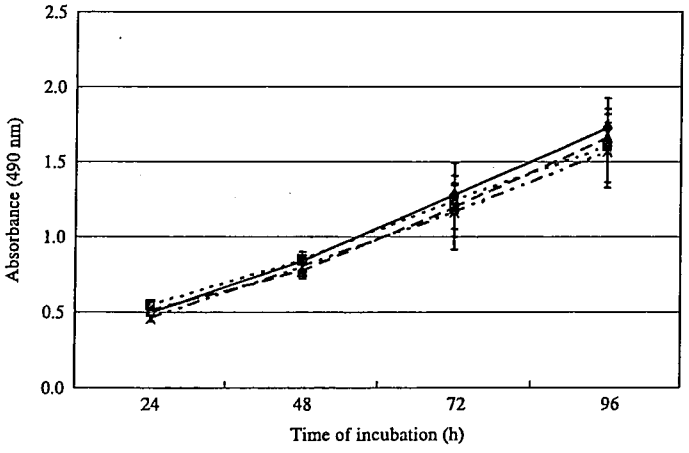

Fig. 4. Assessment of the mitogenicity of the SWKLPPS peptide in AZ-P7a cells. AZ-P7a gastric cancer cells were incubated in 96-well plates at 5×10^3 cells/well in the presence of 1 μM (■), 10 μM (▲) or 100 μM (×) of the SWKLPPS peptide or without the peptide (◆). The cell viability was monitored after 24, 48, 72 and 96 h using the MTS assay. The quantity of the formazan product present was determined by measuring the absorbance at 490 nm using a microplate autoreader.

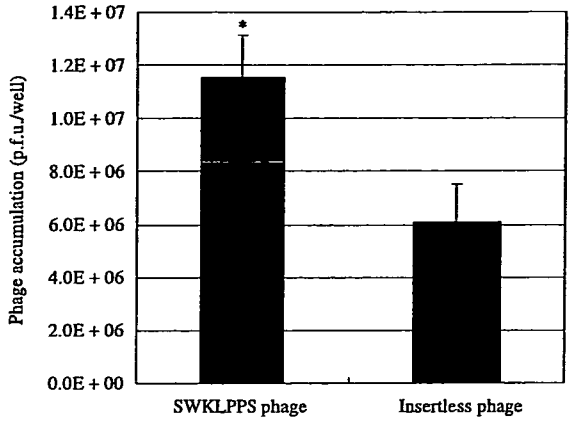

Fig. 5. Binding of the SWKLPPS phage to floating cells in malignant ascites from a patient with gastric cancer. The *ex vivo* binding activity of the SWKLPPS phage to floating cells in malignant ascites from a patient with gastric cancer was examined. The ascites from the patient was concentrated by centrifuge and co-incubated with SWKLPPS phage or insertless phage in 6-well plate. Then the number of phages binding to cells was determined by titering. $^*P < 0.05$ compared to the control.

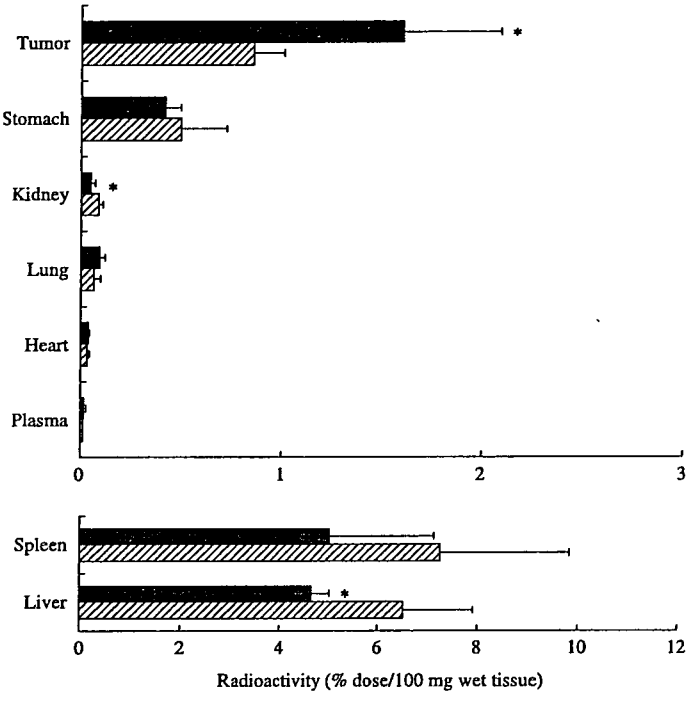

Fig. 6. Biodistribution of SWKLPPS-conjugated liposomes after intraperitoneal injection. Mice with peritoneal metastasis were anesthetized and injected with the radiolabeled liposomes containing [1á,2á(*n*)-^{3}H] cholesterol oleoyl ether with stearoyl 7 mer peptide SWKLPPS (■) or without peptide conjugates (control, ▨) intraperitoneally. The mice were killed 24 h after injection, and blood was collected and centrifuged to obtain plasma. After the mice had been bled, the tumor and normal organs were removed, washed with saline and weighed. The radioactivity in samples was determined with a liquid scintillation counter. Data are represented as the percentage of the injected dose per 100 mg wet tumor tissue or 100 μL plasma. $^*P < 0.05$ compared to the each control.

itself. Contrary to this, if the phage is injected intravenously, the majority of the phages could bind to the mouse-derived microvessels in the tumor rather than to xenografted human cancer cells. This advantage of intraperitoneal injection might have enabled the SWKLPPS phage to bind to cancer cells in ascites from a patient with carcinomatosa peritonitis, despite the fact that SWKLPPS was isolated using an animal study.

doi: 10.1111/j.1349-7006.2006.00291.x
© 2006 Japanese Cancer Association

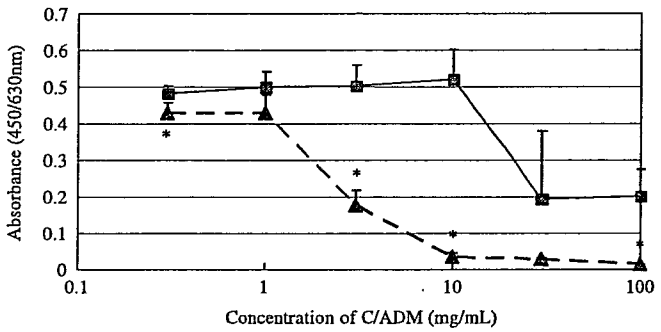

Fig. 7. Anticancer activity of SWK-LipADM. After AZ-P7a cells were plated on a 96-well plate and cultured in a CO_2 incubator at 37°C for 24 h, 20 μL LipADM or SWK-LipADM was added to each well at the ADM concentration of 0.3, 1, 3, 10, 30 and 100 mg/mL and allowed to bind to the cells for 30 min at 37°C. The mediums were changed to RPMI containing 10% FCS and cells were cultured for further 24 h. Cell proliferation assay with TetraColor One was carried out. * $P < 0.01$ compared to LipADM.

The SWKLPPS peptide showed no significant ability to mediate mitogenesis *in vitro* following binding to gastric cancer cells. This is important for application of a novel peptide to actual cancer treatment, as it is undesirable to give potent mitogens to cancer patients. In addition to this safety profile, SWKLPPS has several pharmacological advantages. The majority of targeting ligands in cancer therapy are relatively large proteins and have some pharmacological limitations, notably a short plasma half-life, unwanted interactions with serum components and high costs of manufacture. In contrast, SWKLPPS is a simple peptide with excellent stability and a low manufacturing cost. Furthermore, despite consisting of only seven amino acid residues, SWKLPPS is expected to work sufficiently as a targeting ligand, as peptides containing three amino acid residues, such as RGD, have been reported to provide the minimal framework for structural formation and protein–protein interactions.[23] In fact, the competitive inhibition of SWKLPPS phage binding to peritoneal tumors by the synthesized KLP-containing peptide implies that the synthesized KLP peptide itself has a strong binding activity to peritoneal tumors both *in vitro* and *in vivo*.

Liposomes are one of the promising drug delivery systems for cancer treatment.[24] In this study we developed SWKLPPS-conjugated liposomes and these liposomes accumulated in the tumors significantly more than control liposomes after intraperitoneal injection. Less SWKLPPS liposomes appeared in the intra-abdominal organs compared to the control (significant difference in the liver and kidney). Similar results have been reported after intravenous injection of peptide-modified liposomes in tumor-bearing mice.[25] The reason for this characteristic of peptide-modified liposomes is not clear at present. One possible explanation in our experiment is a subtraction effect in the biopanning procedure. Namely, in the intraperitoneal biopanning, phage-selection for tumors could be regarded as a subtraction process for normal peritoneum covering the surface of organs (e.g., liver and kidney). Therefore it might not be strange that SWKLPPS shows the ability to bind tumors and avoid the normal peritoneum simultaneously. In addition, modification of liposomes with SWKLPPS could enhance the anticancer activity of ADM on AZ-P7a gastric cancer cells. These results encourage us to attempt further investigations to confirm the antitumor effects of SWKLPPS-conjugated anticancer agents *in vivo*, aiming for their application to clinical practice.

Acknowledgments

We thank Professor Toshiki Tanaka for support in the SWKLPPS peptide synthesis, and Professor Koichi Hirata and Dr Takahiro Yasoshima for supplying the AZ-P7a cells. This work was supported by grants from the Japan Society for the Promotion of Science, the Fujita Memorial Fund for Medical Research and the Japan Research Foundation for Clinical Pharmacology.

References

1 Parkin DM, Bray F, Ferlay J, Pisani P. Global cancer statistics, 2002. *CA Cancer J Clin* 2005; **55**: 74–108.
2 Kodera Y, Nakanishi H, Yamamura Y *et al.* Prognostic value and clinical implications of disseminated cancer cells in the peritoneal cavity detected by reverse transcriptase-polymerase chain reaction and cytology. *Int J Cancer* 1998; **79**: 429–33.
3 Sakakura C, Hagiwara A, Nakanishi M *et al.* Differential gene expression profiles of gastric cancer cells established from primary tumour and malignant ascites. *Br J Cancer* 2002; **87**: 1153–61.
4 Sadeghi B, Arvieux C, Glehen O *et al.* Peritoneal carcinomatosis from non-gynecologic malignancies: results of the EVOCAPE 1 multicentric prospective study. *Cancer* 2000; **88**: 358–63.
5 Yanagihara K, Takigahira M, Tanaka H *et al.* Development and biological analysis of peritoneal metastasis mouse models for human scirrhous stomach cancer. *Cancer Sci* 2005; **96**: 323–32.
6 Kashentseva EA, Seki T, Curiel DT, Dmitriev IP. Adenovirus targeting to c-erbB-2 oncoprotein by single-chain antibody fused to trimeric form of adenovirus receptor ectodomain. *Cancer Res* 2002; **62**: 609–16.
7 Fisher KD, Stallwood Y, Green NK, Ulbrich K, Mautner V, Seymour LW. Polymer-coated adenovirus permits efficient retargeting and evades neutralising antibodies. *Gene Ther* 2001; **8**: 341–8.
8 Backer MV, Backer JM. Targeting endothelial cells overexpressing VEGFR-2: selective toxicity of Shiga-like toxin-VEGF fusion proteins. *Bioconjug Chem* 2001; **12**: 1066–73.
9 Lorimer IA, Keppler-Hafkemeyer A, Beers RA, Pegram CN, Bigner DD, Pastan I. Recombinant immunotoxins specific for a mutant epidermal growth factor receptor: targeting with a single chain antibody variable domain isolated by phage display. *Proc Natl Acad Sci USA* 1996; **93**: 14815–20.
10 New England BioLabs Inc. *Ph.D-7 Phage Display Peptide Library Kit: Instruction Manual*. Version 2.7. Beverly: New England Biolabs Inc., 2002.
11 Nishimori H, Yasoshima T, Denno R *et al.* A novel experimental mouse model of peritoneal dissemination of human gastric cancer cells: different mechanisms in peritoneal dissemination and hematogenous metastasis. *Jpn J Cancer Res* 2000; **91**: 715–22.
12 Wong JK, Kennedy PR, Belcher SM. Simplified serum- and steroid-free culture conditions for high-throughput viability analysis of primary cultures of cerebellar granule neurons. *J Neurosci Meth* 2001; **110**: 45–55.
13 Oku N, Doi K, Namba Y, Okuda S. Therapeutic effect of adriamycin encapsulated in long-circulating liposome on Meth-A-sarcoma-bearing mice. *Int J Cancer* 1994; **58**: 415–9.
14 Carter WG, Ryan MC, Gahr PJ. Epiligrin, a new cell adhesion ligand for integrin alpha 3 beta 1 in epithelial basement membranes. *Cell* 1991; **65**: 599–610.
15 Takatsuki H, Komatsu S, Sano R, Takada Y, Tsuji T. Adhesion of gastric carcinoma cells to peritoneum mediated by alpha3beta1 integrin (VLA-3). *Cancer Res* 2004; **64**: 6065–70.
16 Ura H, Denno R, Hirata K, Yamaguchi K, Yasoshima T. Separate functions of alpha2beta1 and alpha3beta1 integrins in the metastatic process of human gastric carcinoma. *Surg Today* 1998; **28**: 1001–6.
17 Maruta F, Parker AL, Fisher KD *et al.* Identification of FGF receptor-binding peptides for cancer gene therapy. *Cancer Gene Ther* 2002; **9**: 543–52.
18 Binetruy-Tournaire R, Demangel C, Malavaud B *et al.* Identification of a peptide blocking vascular endothelial growth factor (VEGF) -mediated angiogenesis. *EMBO J* 2000; **19**: 1525–33.
19 Pasqualini R, Ruoslahti E. Organ targeting *in vivo* using phage display peptide libraries. *Nature* 1996; **380**: 364–6.
20 Arap W, Haedicke W, Bernasconi M *et al.* Targeting the prostate for destruction through a vascular address. *Proc Natl Acad Sci USA* 2002; **99**: 1527–31.
21 Walters RW, Grunst T, Bergelson JM, Finberg RW, Welsh MJ, Zabner J. Basolateral localization of fiber receptors limits adenovirus infection from the apical surface of airway epithelia. *J Biol Chem* 1999; **274**: 10219–26.
22 Arap W, Pasqualini R, Ruoslahti E. Cancer treatment by targeted drug delivery to tumor vasculature in a mouse model. *Science* 1998; **279**: 377–80.
23 Arap W, Kolonin MG, Trepel M *et al.* Steps toward mapping the human vasculature by phage display. *Nat Med* 2002; **8**: 121–7.
24 Hamaguchi T, Matsumura Y, Nakanishi Y *et al.* Antitumor effect of MCC-465, pegylated liposomal doxorubicin tagged with newly developed monoclonal antibody GAH, in colorectal cancer xenografts. *Cancer Sci* 2004; **95**: 608–13.
25 Kondo M, Asai T, Katanasaka Y *et al.* Anti-neovascular therapy by liposomal drug targeted to membrane type-1 matrix metalloproteinase. *Int J Cancer* 2004; **108**: 301–6.

© 2006 Japanese Cancer Association

Available online at www.sciencedirect.com
ScienceDirect
Journal of Controlled Release 118 (2007) 303–309
journal of controlled release
www.elsevier.com/locate/jconrel

Effective tumor regression by anti-neovascular therapy in hypovascular orthotopic pancreatic tumor model

Sei Yonezawa, Tomohiro Asai, Naoto Oku *

Department of Medical Biochemistry and COE Program in the 21st Century, University of Shizuoka School of Pharmaceutical Sciences, 52-1 Yada, Suruga-ku, Shizuoka 422-8526, Japan

Received 10 September 2006; accepted 21 December 2006
Available online 5 January 2007

Abstract

Pancreatic cancer is one of the most serious cancers with poor therapeutic results and prognosis. In here, we proposed a novel treatment strategy of pancreatic cancer by injuring limited angiogenic vessels with liposome containing adriamycin. At first, we established an orthotopic tumor model, which has a hypovascular characteristic of pancreatic tumor. In this model, we obtained the enhanced therapeutic efficacy with liposome that modified by polyethylene glycol (PEG) and a peptide, Ala-Pro-Arg-Pro-Gly (APRPG), having an affinity to neovessels. Histochemical analysis suggested the degradation of angiogenic vessels after treatment with APRPG-PEG-liposomal adriamycin. In addition, we observed colocalization of fluorescence-labeled APRPG-PEG-liposome with angiogenic endothelial cells, although the biodistribution of ^{3}H-labeled liposome did not show the difference in the amount of accumulation between PEG-modified liposome and APRPG-PEG-modified liposome. These results suggested the availability of the anti-neovascular therapy against pancreatic cancer and supply a new sight indication on chemotherapeutics against pancreatic cancer.
© 2007 Elsevier B.V. All rights reserved.

Keywords: Anti-neovascular therapy; Liposome; Pancreatic cancer; Angiogenesis

1. Introduction

Pancreatic cancer is one of the most difficult cancers to control: This cancer is difficult to diagnose, and shows high malignant potential. Five-year survival of patients suffering pancreatic cancer is less than 5% in the United States, Japan and Europe, and the incidence rate of it is equal to the death rate [1]. Therefore, it is suggested that existing chemotherapeutics have a limitation of the effect on pancreatic cancer, and an effective treatment modality is awaited. It is interesting to note that pancreatic cancer has less vasculature in number than other cancers such as breast or colorectal cancer known as vasculature-rich cancers. In computed tomography (CT) and magnetic resonance imaging (MRI), pancreatic tumor is considered as a hypovascular lesion compared to normal pancreatic tissue [2–4]. This property can be thought as the reason why effective pancreatic tumor chemotherapy cannot be expected due to the low bioavailability of the chemotherapeutic drugs.

On the other hand, angiogenic vessels are known to play an important role in pancreatic tumor progression as well as other tumors [5]. In general, anti-angiogenic therapy is thought to be effective for cancer treatment. Actually, many anti-angiogenic therapies that inhibit the certain steps of angiogenesis have examined. For example, matrix metalloproteinase inhibitors and anti-vascular endothelial growth factor (VEGF) agents etc., have been developed [6–8]. However, they are thought to be limited for the induction of tumor dormancy [9,10]. We previously proposed a novel therapeutic strategy targeted angiogenic vessels, cancer anti-neovascular therapy (ANET), that kills the proliferative endothelial cells followed by indirect induction of tumor regression [11,12]. Neovessel endothelial cells are growing, so it can be thought that these cells are susceptible to anti-cancer drugs like tumor cells. The benefits that can be gained from ANET are not only the effective tumor treatment but also the inhibition of tumor hematogenous metastasis, the avoidance of drug resistance, and wide range of application

* Corresponding author. Tel.: +81 54 264 5701; fax: +81 54 264 5705.
E-mail address: oku@u-shizuoka-ken.ac.jp (N. Oku).

0168-3659/$ - see front matter © 2007 Elsevier B.V. All rights reserved.
doi:10.1016/j.jconrel.2006.12.024

against many kinds of tumors. For ANET, we previously isolated APRPG peptide from a phage-displayed peptide library by biopanning of phage clones specifically bound to tumor angiogenic vasculature. *In vitro* study, we observed higher uptake of APRPG-modified liposome in human umbilical vein endothelial cells (HUVECs) than non-modified one. Furthermore, higher accumulation of APRPG-modified liposomes in tumor tissue than non-modified one was also observed in tumor-bearing mice [12].

In here, we carried out a series of experiments focused on the application of ANET to pancreatic tumor model, since it is thought that ANET is more effective in hypovascular tumors than hypervascular tumors. Firstly, we established hypovascular orthotopic pancreatic tumor model, following the investigation of biodistribution of angiogenic vessel-targeted liposome in the tumor-bearing mice. In this experiment, we used APRPG-polyethyleneglycol (PEG)-modified liposome as the angiogenic vessel-targeted liposome. Modification by PEG is known to protect liposomes from opsonization and contact with lipoproteins through the formation of aqueous layers on the surface of liposomes. Thus, the APRPG-PEG-modified liposome could have long-circulating characteristic, and would have more chance to contact with neovasculature. Next, we examined the intratumoral distribution of liposomes by using confocal laser scan microscopy. And finally, we treated the orthotopic pancreatic tumor model with APRPG-PEG-modified liposomes encapsulating adriamycin (ADM) and evaluated the therapeutic effect. The obtained data indicated that ANET is effective for pancreatic tumor treatment.

2. Materials and methods

2.1. Materials

Distearoylphosphatidylcholine (DSPC) and distearoylphosphatidylethanolamine (DSPE) were kindly gifted form Nippon Fine Chemical Co., Ltd. (Hyogo, Japan). PEG-APRPG-conjugated DSPE (DSPE-PEG-APRPG) and PEG-conjugated DSPE (DSPE-PEG) were prepared as described previously [13]. Cholesterol was purchased from Sigma (St. Louis, MO, USA). All other reagents used were the analytical grades.

2.2. Cell culture

Human pancreatic cancer cell line SUIT-2 was generously donated by Dr. Haruo Iguchi (National Kyushu Cancer Center, Fukuoka, Japan). SUIT-2 cells were cultured in RPMI 1640 supplemented with streptomycin, penicillin, and 10% fetal bovine serum (FBS, Sigma) at 37 °C in a humidified atmosphere containing 5% CO_2.

2.3. Orthotopic tumor model

BALB/c nude mice were anesthetized by intraperitoneal injection of pentobarbital (Dainippon Sumitomo Pharmaceutical Co., Ltd. Osaka, Japan). After cutting abdomen of a mouse, pancreas was exteriorized and dilated on its belly sterilized by chlorhexidine gluconate solution. Then 20 μL of SUIT-2 cells (5×10^6 cells/mouse) were injected into pancreas. Then cut area was sutured and sterilized by chlorhexidine gluconate solution.

2.4. Histopathological examination

SUIT-2 cells (5×10^6 cells/mouse) were inoculated as described in the Section 2.3. At day 3 and 9 after tumor implantation, mice were sacrificed and tumor was dissected. The tumor was embedded in optimal cutting temperature compound (Sakura Finetechnochemical Co., Ltd., Tokyo, Japan) and frozen at −80 °C. Nine-micrometer tumor sections were prepared by using cryostatic microtome (HM 505E, Microm, Walldorf, Germany), mounted on MAS coated slides (Matsunami Glass Ind., Ltd., Japan), and air-dried for 1 h. The tumor tissue sections prepared were stained with hematoxylin-eosin and histopathological examination was performed.

2.5. Evaluation of micro vessel density (MVD) in pancreatic tumor model

SUIT-2 cells (5×10^6 cells/mouse) were inoculated as described in the Section 2.3. On the day 10 and 25 after tumor implantation, mice were sacrificed and the tumor section was prepared as described in the Section 2.4. The tumor tissue sections prepared were fixed in acetone for 10 min at room temperature, washed twice with phosphate-buffered saline (PBS), pH 7.4, (5 min each time), and incubated with protein-blocking solution containing 1% bovine serum albumin in PBS for 10 min at room temperature. Then, the samples were incubated with an appropriately diluted (1:50) biotinylated anti-mouse CD31 rat monoclonal antibody (Becton Dickinson Lab., Franklin Lakes, NJ, USA) for 18 h at 4 °C. After the sections were rinsed thrice (2 min each time) with PBS, they were incubated with streptavidin-Alexa fluor® 488 conjugates (Molecular Probes Inc., Eugene, OR, USA) for 30 min at room temperature in a humid chamber. Samples were washed twice with PBS (2 min each time). Finally, sections were counterstained and mounted with Perma Fluor Aqueous Mounting Medium (Thermo Shandon, Pittsburgh, PA, USA). These sections were fluorescently observed by using microscopic LSM system (Carl Zeiss, Co., Ltd.): Endothelial cells were identified as green fluorescence. Hot spot area of the samples and CD31 positive area were quantified by ImageJ software to obtain micro vessel density (MVD). For immunostaining, the sections treated with biotinylated anti-mouse CD31 rat monoclonal antibody were stained with VECTASTAIN® ABC Kit (Vector Laboratories, Inc., Burlingame, CA, USA) by using diaminobenzidine tetrahydrochloride (DAB, Funakoshi Co., Ltd., Tokyo, Japan) as a colorimetric substrate. Then the sections were rinsed with PBS and co-stained with hematoxylin.

2.6. Preparation of liposomes

Liposomes composed of DSPC and cholesterol with DSPE-PEG or DSPE-PEG-APRPG (10:5:1 as a molar ratio, PEG-Lip and APRPG-PEG-Lip, respectively) were prepared as described